REPORT 1151

THE EFFECTS ON DYNAMIC LATERAL STABILITY AND CONTROL OF LARGE ARTIFICIAL VARIATIONS IN THE ROTARY STABILITY DERIVATIVES[1]

By Robert O. Schade and James L. Hassell, Jr.

SUMMARY

An investigation has been conducted in the Langley free-flight tunnel to determine the effects of large artificial variations of several rotary lateral-stability derivatives on the dynamic lateral stability and control characteristics of a 45° sweptback-wing airplane model. The derivatives investigated were the damping-in-yaw derivative C_{n_r} (the yawing moment due to yawing), the damping-in-roll derivative C_{l_p} (the rolling moment due to rolling), and the two cross derivatives C_{l_r} (the rolling moment due to yawing) and C_{n_p} (the yawing moment due to rolling). Flight tests of a free-flying model were made in which the derivatives were varied over a wide range by means of an artificial-stabilization device incorporating a gyroscope sensitive to rolling or yawing velocity. Calculations of the period and damping of the lateral motions and of the response to roll and yaw disturbances were made for correlation with the experimental results. In order to simplify the analysis, most of the calculations were based on the assumption of idealized artificial-stabilization systems, but a few check calculations were made in which the small constant time lag of the stabilization device used in the tests was taken into account. Extensive calculations were not made by this method, however, because of the extremely laborious process involved and because a systematic determination of the effect of time lag on stability throughout the variation of the four derivatives was considered beyond the scope of the present investigation.

The calculated results were in qualitative agreement with the experimental results in predicting the general trends in flight characteristics produced by large changes in the stability derivatives, but in some cases the theory with the assumption of zero lag was not in good quantitative agreement with the experimental results. In these cases the check calculations with time lag taken into account indicated that the discrepancies could be attributed to the effect of the small constant time lag in the stabilization device used. The results showed that the only derivative which provided a large increase in damping of the lateral oscillation without adversely affecting other flight characteristics was C_{n_r}. (Because of the limitations imposed by the relatively small size of the test section of the Langley free-flight tunnel, however, the flight characteristics of the model were not appreciably influenced by the stiffness in turning maneuvers that has been found objectionable in some airplanes equipped with yaw dampers.)

Increasing C_{l_p} to moderately large negative values produced substantial increases in the damping of the lateral oscillation but caused an objectionable stiffness in roll. Further negative increases in C_{l_p} did not cause additional increases in damping of the lateral oscillation and made the stiffness in roll more objectionable. Increases in C_{l_r} or C_{n_p} in the positive direction produced an increase in damping of the lateral oscillation but caused an undesirable spiral tendency.

INTRODUCTION

Many present-day high-speed airplanes have exhibited unsatisfactory damping of the lateral oscillation, partly because of the configurations required for high-speed flight and partly because of the more severe operating conditions encountered (high altitude and high wing loading). Since in many cases satisfactory oscillatory stability cannot be obtained by making reasonable geometric changes to the airplane, much interest has been shown in the use of artificial-stabilization devices as a means of obtaining satisfactory damping of the lateral oscillation.

Yaw dampers have been installed in some airplanes in an effort to improve the lateral oscillatory stability. This artificial-stabilization device provides rudder deflection in response to a signal from a gyroscope sensitive to yawing velocity so that the yawing moment of the rudder tends to damp the lateral motion of the airplane. In an idealized system such a device produces the damping-in-yaw derivative C_{n_r} (the yawing moment due to yawing). Similar devices can be considered, in an idealized case, to vary the damping-in-roll derivative C_{l_p} (the rolling moment due to rolling) and the two cross derivatives C_{n_p} (the yawing moment due to rolling) and C_{l_r} (the rolling moment due to yawing). In a practical case, of course, the actual characteristics of the artificial-stabilization device should be taken into account rather than considering that the device produces a simple change in one of these derivatives. References 1 and 2 present some results of theoretical investigations of large derivative variations as produced by idealized artificial-stabilization systems and references 3 and 4 present methods for taking into account the effect of constant time lag in the stabilization systems.

[1] Supersedes NACA TN 2781, "The Effects on Dynamic Lateral Stability and Control of Large Artificial Variations in the Rotary Stability Derivatives" by Robert O. Schade and James L. Hassell, Jr., 1952.

321605—55——63

Varying the value of either of the damping derivatives C_{n_r} and C_{l_p} changes the total damping of the airplane. Varying the value of either of the cross derivatives C_{n_p} and C_{l_r} primarily causes a redistribution of the natural damping of the system for cases in which the airplane has low values of the product of inertia. For high values of the product of inertia, variations in C_{n_p} or C_{l_r} can cause sizable changes in the total damping of the airplane.

In order to study the relative effects of large independent variations of these four rotary stability derivatives on the dynamic stability and control characteristics of airplanes, an investigation has been carried out in the Langley free-flight tunnel on a free-flying dynamic airplane model equipped with an artificial-stabilization device incorporating a rate-sensitive gyroscope. This investigation is a part of a general research program to determine the effects of several of the lateral-stability derivatives, both independently and in combination, on dynamic lateral stability and control.

Force tests were made to determine all the lateral-stability derivatives of the model in the basic condition for use in making calculations and establishing flight-test conditions. Calculations were made to determine the period and damping of the lateral motions and the lateral response to rolling and yawing disturbances for correlation with flight-test results. In order to simplify the analysis, most of the calculations were based on the assumption of idealized artificial-stabilization systems although the stabilization device used in the tests did have a small constant time lag. Additional calculations including the effect of constant time lag were made for some conditions in which the idealized theory was not in good quantitative agreement with the experimental results. All tests and calculations were made at a lift coefficient of 1.0.

Although the results do not apply directly to airplanes or flight conditions other than those investigated, the trends of the results presented are believed to give a qualitative indication of the general effects of large independent variations of the four stability derivatives under consideration.

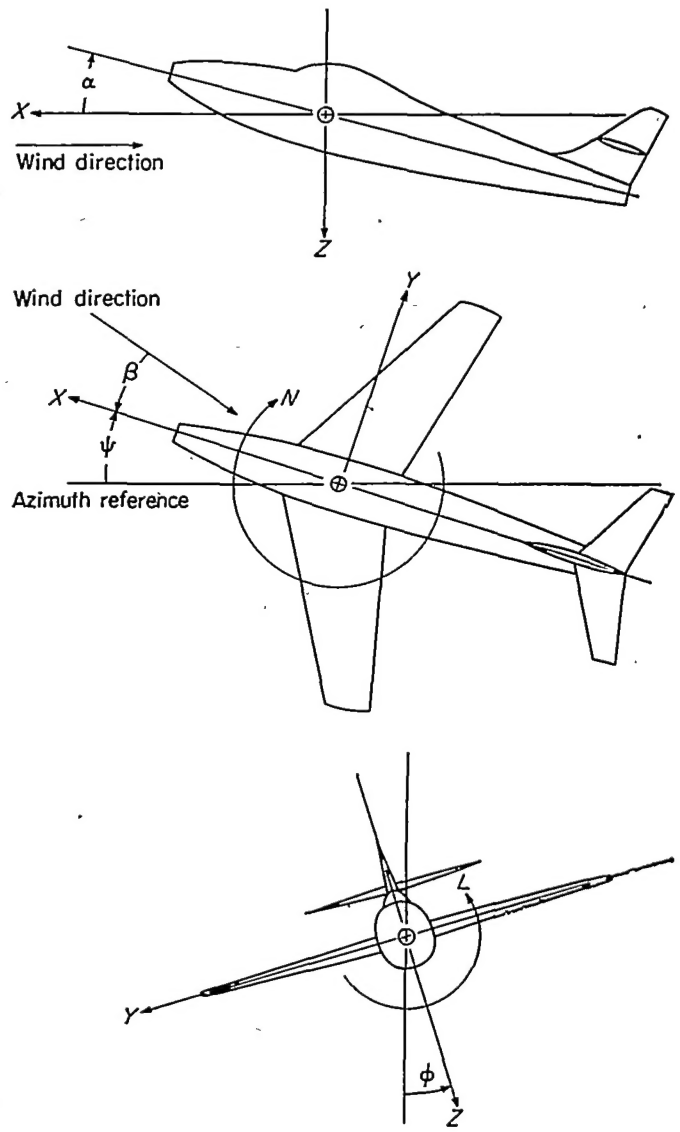

FIGURE 1.—The stability system of axes. Arrows indicate positive directions of moments, forces, and angles. This system of axes is defined as an orthogonal system having the origin at the center of gravity and in which the Z-axis is in the plane of symmetry and perpendicular to the relative wind, the X-axis is in the plane of symmetry and perpendicular to the Z-axis, and the Y-axis is perpendicular to the plane of symmetry. At a constant angle of attack, these axes are fixed in the airplane.

SYMBOLS AND COEFFCIENTS

All force and moment measurements were obtained with respect to the stability axes. A sketch showing the axes and the positive directions of the forces, moments, and angles is given in figure 1.

C_L	lift coefficient, Lift/qS
C_n	yawing-moment coefficient, Yawing moment/qSb
C_l	rolling-moment coefficient, Rolling moment/qSb
C_Y	lateral-force coefficient, Lateral force/qS
L	rolling moment, about X-axis, ft-lb
N	yawing moment, about Z-axis, ft-lb
Y	lateral force, lb
q	dynamic pressure, $\frac{1}{2}\rho V^2$, lb/sq ft
S	wing area, sq ft
l	distance from airplane center of gravity to vertical-tail center of pressure, ft
b	wing span, ft
t	time, sec
y	sidewise displacement from center line of test section, ft
ρ	mass density of air, slugs/cu ft
V	airspeed, ft/sec
β	angle of sideslip, radians except where otherwise noted
ψ	angle of yaw, deg
ϕ	angle of bank, deg
α	angle of attack, deg
δ	control deflection, deg
δ_a	total aileron deflection, deg

δ_t vertical-tail deflection, deg

μ relative density factor, $m/\rho Sb$

m mass of airplane, slugs

η angle of attack of principal longitudinal axis of airplane, deg

ω frequency, radians/sec

ω_0 natural frequency of model, radians/sec

δ_a/p amplitude ratio, $\frac{\text{Aileron deflection}}{\text{Rolling velocity}}$, deg/radian/sec

γ inclination of flight path to horizontal axis, positive in a climb, deg

I_{x_0} moment of inertia about principal longitudinal axis, slug-ft^2

I_{z_0} moment of inertia about principal normal axis, slug-ft^2

k_{x_0} radius of gyration in roll about principal longitudinal axis, ft

k_{z_0} radius of gyration in yaw about principal vertical axis, ft

K_X nondimensional radius of gyration in roll about longitudinal stability axis,

$$\sqrt{\left(\frac{k_{X_0}}{b}\right)^2 \cos^2\eta+\left(\frac{k_{Z_0}}{b}\right)^2 \sin^2\eta}$$

K_Z nondimensional radius of gyration in yaw about vertical stability axis,

$$\sqrt{\left(\frac{k_{Z_0}}{b}\right)^2 \cos^3\eta+\left(\frac{k_{X_0}}{b}\right)^2 \sin^2\eta}$$

K_{XZ} nondimensional product-of-inertia parameter,

$$\left[\left(\frac{k_{Z_0}}{b}\right)^2-\left(\frac{k_{X_0}}{b}\right)^2\right]\sin\eta\cos\eta$$

i_w wing incidence, deg

$pb/2V$ rolling-angular-velocity factor, radians

$rb/2V$ yawing-angular-velocity factor, radians

p rolling angular velocity, radians/sec

r yawing angular velocity, radians/sec

$$C_{Y_\beta}=\frac{\partial C_Y}{\partial\beta}$$

$$C_{n_\beta}=\frac{\partial C_n}{\partial\beta}$$

$$C_{l_\beta}=\frac{\partial C_l}{\partial\beta}$$

$$C_{l_p}=\frac{\partial C_l}{\partial\frac{pb}{2V}}$$

$$C_{Y_p}=\frac{\partial C_Y}{\partial\frac{pb}{2V}}$$

$$C_{n_p}=\frac{\partial C_n}{\partial\frac{pb}{2V}}$$

$$C_{n_r}=\frac{\partial C_n}{\partial\frac{rb}{2V}}$$

$$C_{Y_r}=\frac{\partial C_Y}{\partial\frac{rb}{2V}}$$

$$C_{l_r}=\frac{\partial C_l}{\partial\frac{rb}{2}}$$

$$(C_l)_{\delta_a}=\frac{\partial C_l}{\partial\delta_a}$$

$$(C_n)_{\delta_t}=\frac{\partial C_n}{\partial\delta_t}$$

C_{l_c} rolling-moment coefficient due to deflection of both ailerons

C_{n_c} yawing-moment coefficient due to rudder deflection

P period of oscillation, sec

$T_{1/2}$ time for amplitude of lateral oscillation or aperiodic mode of motion to decrease to one-half amplitude, sec

A, B coefficients of first two terms of lateral-stability quartic equation (see ref. 1)

$$\frac{B}{A}=-\frac{1}{4\mu}\frac{\left[\begin{array}{c}2K_X^2K_Z^2C_{Y_\beta}+K_X^2C_{n_r}+K_Z^2C_{l_p}-\\2K_{XZ}^2C_{Y_\beta}-K_{XZ}C_{l_r}-K_{XZ}C_{n_p}\end{array}\right]}{K_X^2K_Z^2-K_{XZ}^2}$$

APPARATUS

TUNNEL AND MODEL

The flight-test part of the investigation was carried out in the Langley free-flight tunnel which is equipped for testing free-flying dynamic models. A complete description of the tunnel and its operation is given in reference 5. The static longitudinal and lateral stability characteristics were determined in the Langley stability tunnel and the aileron- and rudder-effectiveness tests were made in the Langley free-flight tunnel. The dynamic lateral-stability derivatives were determined in the Langley stability tunnel by the yawing- and rolling-flow techniques described in references 6 and 7.

A three-view drawing of the model used in the investigation is presented in figure 2 and a photograph of the model is presented as figure 3. The dimensional and mass characteristics of the model are presented in table I. A wing having 45° sweepback of the leading edge, a taper ratio of 0.5, and an aspect ratio of 3.00 was incorporated in the design because this plan form was typical of a number of proposed fighter airplanes. The center of gravity of the model was located at 23.3 percent of the mean aerodynamic

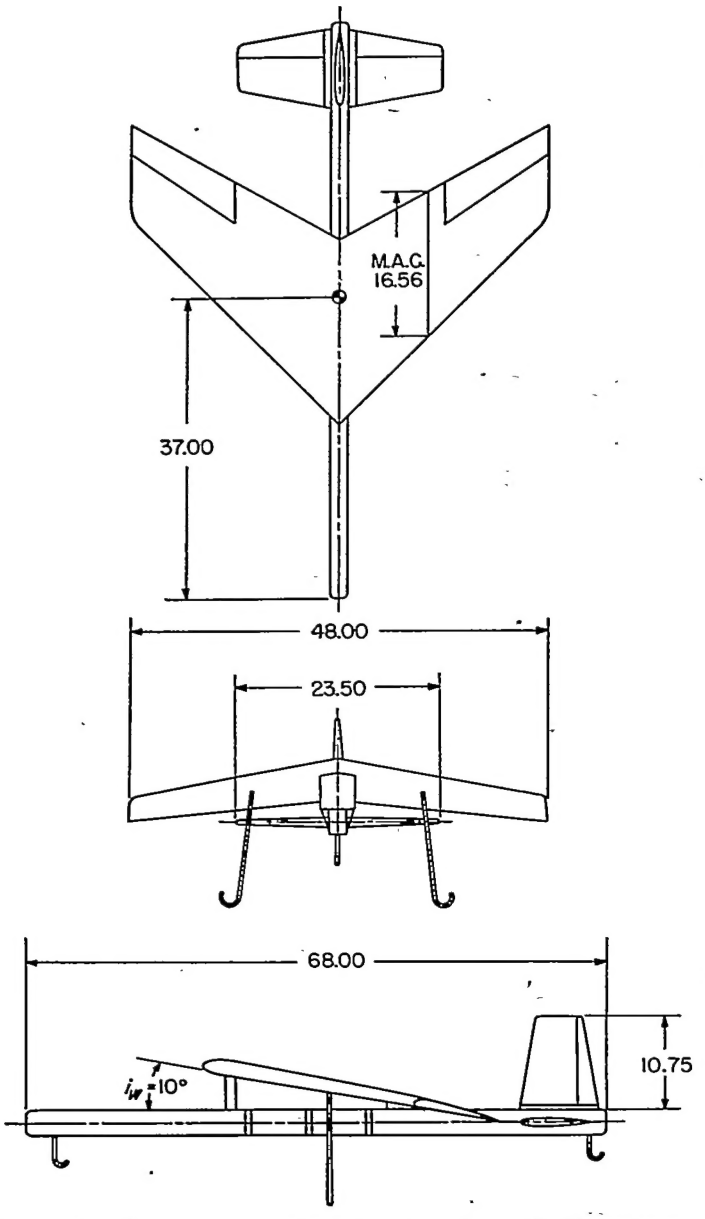

FIGURE 2.—Three-view drawing of test model. All dimensions are in inches.

chord for all tests. The model was equipped with oversize (half-span, 30-percent-chord) ailerons and an all-movable vertical tail in order to obtain the high rolling and yawing moments required for large variations of the rotary derivatives. The ailerons were also used for manual control but the all-movable tail had a flap-type rudder for manual control. Conventional horizontal stabilizing surfaces were employed. A boom-type metal fuselage was used in order to simplify the construction of the model.

For manual control the rudder and ailerons were electrically interconnected to move together in order to eliminate the adverse yawing moment of the ailerons. Aileron and rudder deflections of ±21° and ±14°, respectively, were used for all flight conditions except for the highest value of C_{l_p}. In this condition the aileron deflection was ±29° and the rudder deflection was ±19°.

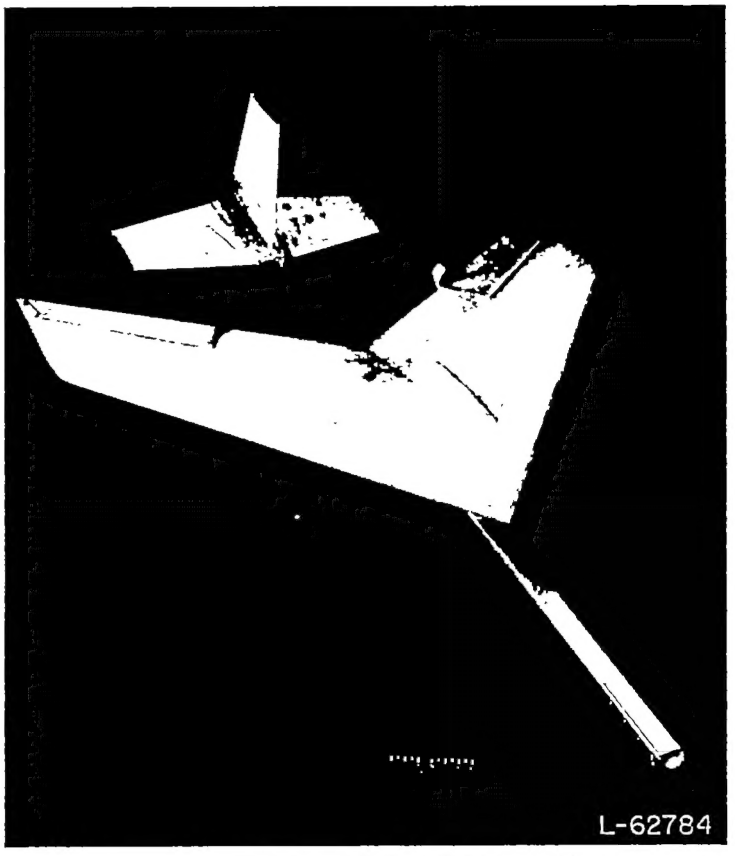

FIGURE 3.—Model used in free-flight tunnel tests.

The manually controlled rudder was operated by a flicker-type (full on or full off) electrical actuator. Although all other servoactuators were of the proportional pneumatic type, essentially flicker-type control was obtained with them because control was applied by abrupt movements of the control sticks and because very high gearing was used between the stick and control surface.

In order to have the model represent an airplane that had poor oscillatory stability and hence require an artificial-stabilization device, the wing incidence was adjusted so that the basic model had a neutrally stable lateral oscillation at the test lift coefficient of 1.0. This neutrally stable oscillation was obtained by increasing the wing incidence to 10° so that the principal axes of inertia became more closely alined with the wind axes. (See ref. 8.)

ARTIFICIAL-STABILIZATION DEVICE

The artificial-stabilization device used in this investigation consisted of a rate gyro and a servoactuator. The rate gyro was mounted on a quadrant so that it could be alined with either the roll or yaw stability axis; therefore it would be sensitive only to a rolling or a yawing velocity as desired. The servoactuator operated both the ailerons and the all-movable tail to produce the derivatives C_{l_p} or C_{l_r}. In order to produce pure rolling moments without adverse yaw, the all-movable tail had to be deflected simultaneously with the ailerons. For the two yawing-moment derivatives C_{n_p} and C_{n_r} the servoactuator operated only the all-movable tail.

TABLE I

DIMENSIONAL AND MASS CHARACTERISTICS OF THE MODEL

Weight, lb	20.5
Wing loading, lb/sq ft	3.85
Relative density factor, $m/\rho Sb$	12.58
Moments of inertia:	
I_{x_0}, slug-ft^2	0.220
I_{z_0}, slug-ft^2	1.473
Wing:	
Airfoil section	Rhode St. Genese 35
Area, sq ft	5.33
Span, ft	4.00
Sweepback, leading edge, deg	45
Incidence, deg	10
Dihedral, deg	0
Taper ratio	0.5
Aspect ratio	3.00
Mean aerodynamic chord, ft	1.38
Location of leading edge of mean aerodynamic chord behind leading edge of root chord, ft	0.99
Root chord, ft	1.78
Tip chord, ft	0.89
Aileron:	
Area (total), percent wing area	12.5
Span (total), percent wing span	50
Chord, percent wing chord	30
Vertical tail:	
Area:	
Square feet	0.53
Percent wing area	10
Span, ft	0.90
Aspect ratio	1.50
Sweepback, 50 percent chord, deg	0
Root chord, ft	0.75
Tip chord, ft	0.44
Tail length (from 0.23 mean aerodynamic chord of wing to 0.25 mean aerodynamic chord of tail), l/b	0.514
Airfoil section	NACA 0009
Horizontail tail:	
Area:	
Square feet (including area through fuselage)	1.19
Percent wing area	22.3
Span, ft	1.96
Aspect ratio	3.23
Sweepback, 50 percent chord, deg	0
Root chord, ft	0.75
Tip chord, ft	0.44
Tail length (from 0.23 mean aerodynamic chord of wing to 0.25 mean aerodynamic chord of tail), l/b	0.514
Airfoil section	NACA 0009
Fuselage:	
Length, ft	5.67
Cross section, in.	2 by 3

No accompanying aileron deflection was required since at the flight-test lift coefficient of 1.0 the tail produced no rolling moment.

Deflection of the all-movable vertical tail to produce the rolling- and yawing-moment derivatives also produced changes in the lateral-force derivatives C_{Y_p} (the lateral force due to rolling) and C_{Y_r} (the lateral force due to yawing). In the calculations, however, these changes in C_{Y_p} and C_{Y_r} were neglected because preliminary calculations indicated that even the largest changes in these derivatives did not appreciably affect the calculated results.

The value of a derivative was artificially increased or decreased by varying the gyro rotor speed or the control linkage to produce more or less control deflection for a given rolling or yawing velocity. The sign of a derivative was changed by rotating the gyro 180° about the rotor axis to give opposite response for a given velocity.

A schematic drawing of the control system used for the C_{l_p} derivative is shown in figure 4. Both ailerons were used for control but for clarity in the drawing only one aileron is shown. This drawing shows the artificial-stabilization device, the manual servoactuator, and the control linkage. This linkage allowed both the artificial-stabilization device and manual actuator to operate the same aileron surfaces. The tubes shown in figure 4 supply air to the gyro rotor to produce a given rotor speed and to the servoactuators to provide the force required to move the control surfaces. Air is also supplied to the gyro pick-off valve which varies the signal pressure to the servoactuator.

In order to explain the operation of the artificial-stabilization device, the assumptions are made that the device is set up to produce negative C_{l_p} and that the model has received a rolling disturbance causing the model to roll to the right. The operation then is as follows: In response to the rolling velocity the rate-gyro rotor produces a torque about the precessional axis of the gyro and the resulting rotation about this axis causes the pick-off valve to move. The movement of the valve varies the signal pressure to the servoactuator which deflects the control surfaces. This control deflection produces a rolling moment which tends to prevent the model from rolling to the right.

An example of the results obtained from the calibration of the artificial-stabilization device is shown in figure 5. The results presented, which are for one value of the derivative C_{l_p}, show the variation of the amplitude ratio and the phase angle with frequency. These results indicate that the amplitude ratio did not vary appreciably throughout the frequency range, but the variation of phase angle with frequency was such that the system had an essentially constant time lag of about 0.05 second.

DETERMINATION OF BASIC STABILITY AND CONTROL PARAMETERS OF THE MODEL

The stability derivatives of the model in the basic condition for a lift coefficient of 1.0 were determined from force tests made at a dynamic pressure of 25 pounds per square foot, which corresponds to a test Reynolds number of approximately 1,245,000 based on the mean aerodynamic chord of 1.38 feet. The results of these tests are given in table II.

Aileron and rudder effectiveness at a lift coefficient of 1.0 was determined from force tests made at a dynamic pressure of 3.0 pounds per square foot which corresponds to a test Reynolds number of approximately 350,000 based on the mean aerodynamic chord of 1.38 feet. The results of these tests showed that for the range of deflections used in

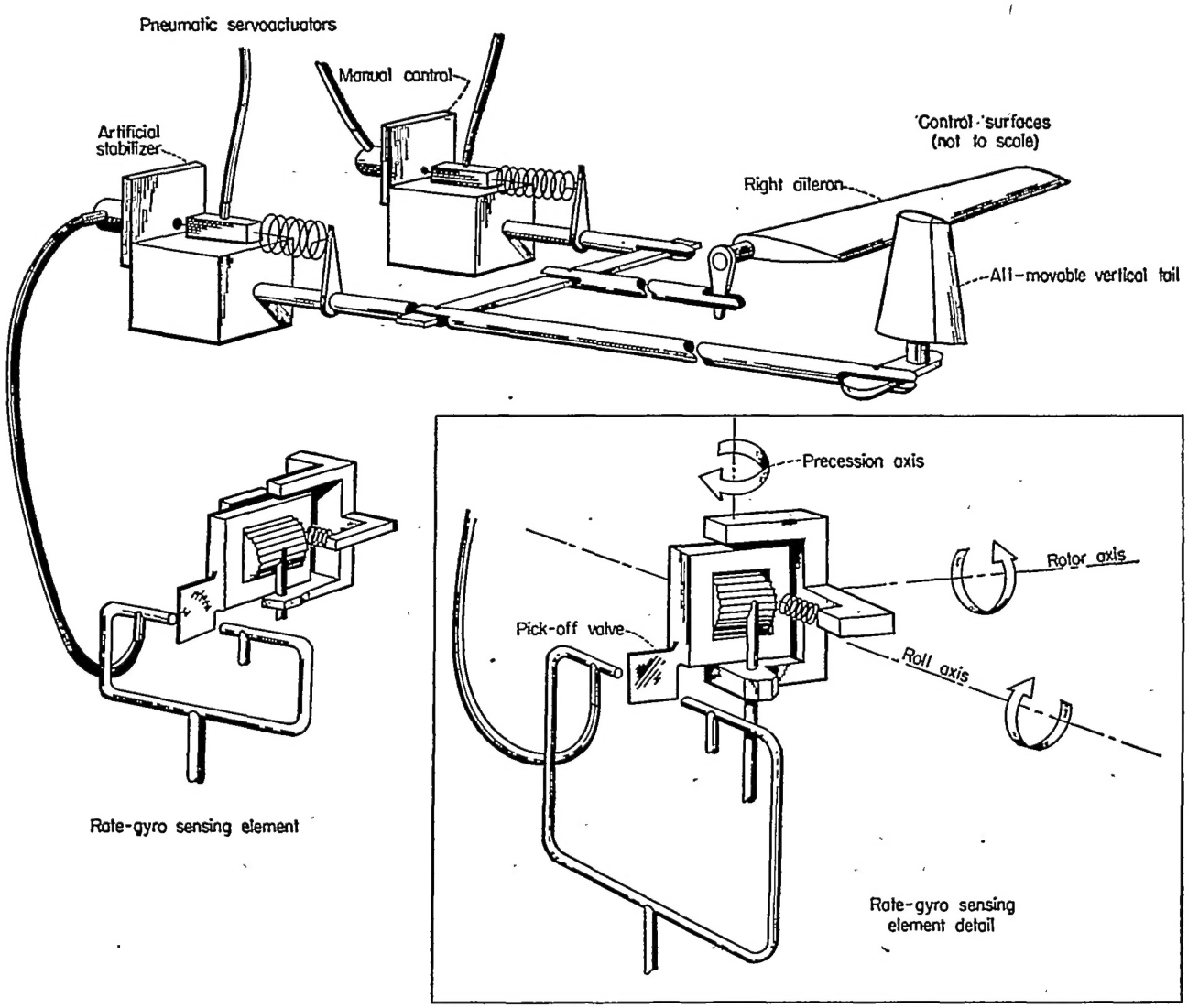

FIGURE 4.—Sketch of artificial-stabilization system. Arrangement for producing C_{l_p} is shown.

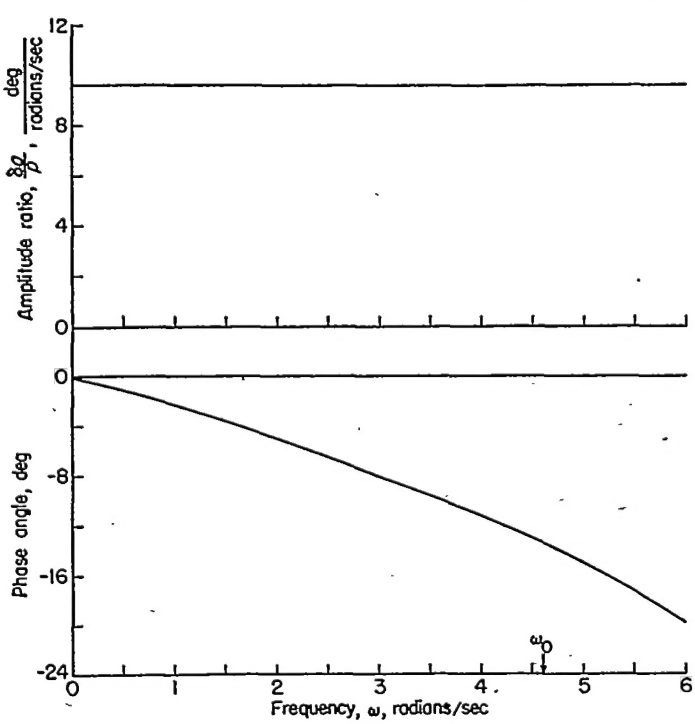

FIGURE 5.—Example of frequency-response data for artificial-stabilization device. (Case shown is for $C_{l_p}=-1.0$.)

the flight tests the variation of control moment with control deflection was linear. The ailerons produced a value of $(C_l)_{\delta_a}$ of 0.0018 per degree and the all-movable tail produced a value of $(C_n)_{\delta_t}$ of 0.0018 per degree. These data were used in determining the values of the stability derivatives simulated by the artificial-stabilization device.

FLIGHT TESTS

TEST PROCEDURE AND RATINGS OF FLIGHT CHARACTERISTICS

The various flight characteristics rated in the free-flight-tunnel tests were the damping of the lateral oscillation, apparent spiral stability, apparent damping in roll, maneuverability, controllability, and general flight behavior. The ratings are listed and defined in table II. These ratings merely indicate the relative effect of changes in the various derivatives on the flight characteristics and should not be considered as absolute ratings that can be used to relate these results with results for other models or full-scale airplanes. Motion-picture records were also obtained to supplement the flight ratings. One of the main uses of these records was to provide time histories for measuring quantitative values of damping.

Control-fixed oscillations were initiated by rocking the model in roll approximately in phase with the natural frequency of the oscillation. This procedure is different from

TABLE II

FLIGHT RATINGS AND CALCULATED PERIOD AND TIME TO DAMP TO ONE-HALF AMPLITUDE FOR FLIGHT-TEST CONDITIONS

Constant Aerodynamic and Mass Terms Used in Calculating the Damping and Period of the Model

μ	12.58	C_L	1.0
$(l/x_f/b)^2$	0.0216	C_{Y_β}	−0.78
$(l/z_f/b)^2$	0.1443	C_{Y_p}	0.31
η	4.68	C_{Y_r}	0.43
K_X^2	0.0225	$\tan\gamma$	−0.2126
K_Z^2	0.1439	C_{n_β}	0.2064
K_{XZ}	0.0100	C_{l_β}	−0.2180
V, ft/sec	56.3		

Explanation of Flight Ratings

Rating		Damping of oscillatory and nonoscillatory motions	Lateral control		General flight behavior
			Maneuverability	Controllability	
A	Satisfactory	Stable; heavily damped	Good	Good	Good.
B		Stable; moderately damped	Fair	Fair	Fair.
C	Unsatisfactory	Stable; lightly damped	Poor	Poor	Poor.
D		Neutrally stable	Very poor	Uncontrollable	Unflyable.
E		Unstable			

Derivative varied	Case	Value of derivative varied	Calculated values for—				Flight ratings for—					
			Oscillatory mode		Aperiodic mode		Damping of lateral oscillation	Damping of the nonoscillatory motion		Maneuverability	Controllability	General flight behavior
			Period, sec	$T_{1/2}$, sec	Spiral $T_{1/2}$, sec	Rolling $T_{1/2}$, sec		Apparent spiral tendency	Apparent damping in roll			
C_{n_r}	1	−7.2	2.25	−8.68	0.05	0.12	E+	A+	B	A−	B+	C−
	2	−5.2	2.22	8.18	.09	.10	C	A+	B	A−	A−	B−
	3	−3.2	2.09	1.51	----------	---------	B	A+	B	A−	A+	A
			3.15	.14								
	4	−2.2	1.84	.88	----------	----------	B+	A	B	A−	A	A−
			5.72	.19								
	5	−1.2	1.50	1.18	.57	.15	B	B+	B	A−	A−	B
	6	−.7	1.42	2.33	1.15	.14	C	B	B	A	B+	B−
	7	[a]−.21	1.37	−24.80	5.02	.14	D	C	B	A	B	C
	8	.0	1.40	−4.76	44.20	.14	D−	D+	B	A	B−	C
	9	1.8	1.43	−.51	−.48	.13	E−	E−	B	A+	C−	D
C_{l_p}	10	−7.3	1.63	1.56	5.09	.01	B	C	A+	D+	A+	C−
	11	−1.3	1.64	1.52	5.44	.04	B	C	A+	C	A+	C
	12	−.8	1.54	1.69	5.31	.07	B	C	A	B	A	B
	13	−.6	1.46	2.35	5.20	.09	B	C	A−	B+	A	B−
	14	−.5	1.42	3.47	5.14	.11	B−	C	B+	A−	A−	B−
	7	[a]−.32	1.37	−24.80	5.02	.14	D	C	B	A	B	C
	15	.1	1.38	−.59	4.21	.33	E	C−	C	A+	C−	C−
C_{l_r}	16	−2.9	1.35	−.40	----------	---------	E	A+	B	A+	C+	C−
			4.40	.24								
	17	−.9	1.38	−1.16	.65	.16	E+	B+	B	A+	B−	C
	7	[a].13	1.37	−24.80	5.02	.14	D	C	B	A	B	C
	18	.3	1.37	13.28	35.40	.14	D+	D	B	[b]	B	C+
	19	1.1	1.36	6.63	−12.31	.13	C	E	B	[b]	C	C
	20	3.1	1.31	.57	−.49	.10	B+	E−	B	[b]	D+	D+
C_{n_p}	21	−.7	1.10	−.73	5.41	.11	E−	C	B	A+	C	C−
	7	[a]−.07	1.37	−24.80	5.02	.14	D	C	B	A	B	C
	22	.0	1.41	7.05	4.97	.16	C	C−	B	A	B+	C+
	23	.3	1.81	.70	4.17	.21	B+	D	B−	[b]	A−	B−
	24	.4	2.00	.44	3.52	.32	A	E	C+	[b]	B	C+
	25	.9	1.56	.19	−.43	8.36	A+	E−	C	[b]	C−	D+

[a] Basic condition.
[b] No definite estimate of maneuverability could be made; see "Results and Discussion" section.

the normal full-scale flight-testing procedure in which the airplane is released from a sideslipped attitude or disturbed by an abrupt rudder deflection. Because of the limited size of the test section in the free-flight tunnel, the model usually struck the tunnel wall after a sideslip disturbance before enough cycles of an oscillation could be obtained for determining the damping.

Apparent spiral stability is a measure of the ability of the model to fly, controls fixed, without an aperiodic divergence into the tunnel wall. One indication of spiral instability in the flight tests was the necessity for almost continuous corrective control to prevent an aperiodic divergence into the tunnel wall. Apparent damping in roll is the measure of the stiffness in roll of the model in response to aileron control.

In this investigation maneuverability is considered a measure of the ability to maneuver the model with aileron control easily and quickly. Controllability is a measure of the ease with which the model can be kept flying satisfactorily in a wings-level attitude.

The general flight behavior is an indication of the overall flight characteristics as affected by all the various stability and control characteristics. A proper balance of oscillatory and aperiodic stability, controllability, and maneuverability is necessary to give satisfactory flying characteristics. The general-flight-behavior ratings are therefore considered the best basis for judging the relative merit of the various flight-test conditions.

RANGES OF VARIABLES

All flight tests were made at a lift coefficient of 1.0 and a wing loading of 3.85 pounds per square foot which corresponds to a value for the relative density parameter μ of 12.58 at sea level. The ranges of values of the four artificially varied

derivatives for which flight tests were made are given in the following table:

Derivative	Value for model in basic condition	Range tested
C_{n_r}	−0.21	−7.2 to 1.8
C_{l_p}	−.32	−7.3 to .1
C_{l_r}	.13	−2.9 to 3.1
C_{n_p}	−.07	−.7 to .9

The values of the derivatives for the model in the basic condition were determined from force tests to an accuracy of two decimal places. For the artificial variation of the derivatives, however, the values could be determined to an accuracy of only one decimal place.

CALCULATIONS

Most of the calculations were made, time lag being neglected, by the method of reference 1 to determine the effects of large variations of the four derivatives on period and damping for the flight-test conditions listed in table II. The mass and aerodynamic parameters used in the calculations are also listed in table II.

For certain conditions in which the experimental and calculated results were not in good quantitative agreement, additional calculations were made in which the effect of time lag in the artificial-stabilization device was considered. These calculations were made for a constant time lag of 0.05 second by the method of reference 3. Extensive calculations were not made by this method, however, because of the extremely laborious process involved and because a systematic determination of the effect of time lag on stability throughout the variation of the four derivatives was considered beyond the scope of the present investigation.

The damping of both the oscillatory and aperiodic motions is expressed in terms of the damping factor $1/T_{1/2}$, the reciprocal of the time to damp to one-half amplitude. Positive values of this damping factor indicate stability and negative values indicate instability (or time to double amplitude). Calculations of motions were also made by the method of reference 9 on a Reeves Electronic Analog Computer for some representative flight-test conditions (table II) to determine the response to a rolling- or a yawing-moment disturbance of 0.01. In these motion calculations the disturbance was applied in one direction for approximately one-half the calculated period of the oscillation and then applied in the opposite direction for an equal length of time.

RESULTS AND DISCUSSION

PRESENTATION OF RESULTS

The experimental results are presented primarily in the form of ratings for the dynamic stability, control, and general flight behavior based on the pilot's comments and, in some cases, these ratings are supplemented by time histories of the motions of the model taken from motion-picture records.

The experimental and calculated results are presented in figures 6 to 17. The flight ratings are presented in table II and examples of time histories showing the changes in the flight characteristics of the model throughout the variation of each derivative are presented in figures 6, 9, 12, and 15.

The calculated dynamic lateral stability characteristics of the model for the range of each derivative covered in the investigation are presented in figures 7, 10, 13, and 16 in the form of period and damping of the lateral oscillation and damping of the aperiodic or nonoscillatory modes of motion. Experimental values of period and damping of the short-period lateral oscillation determined from the flight-test records are also shown in these figures for comparison with the theoretical results. The damping of both the oscillatory motion and the aperiodic motion is expressed in terms of the damping factor $1/T_{1/2}$.

The calculated response of the model to rolling and yawing disturbances for various values of each derivative is presented in figures 8, 11, 14, and 17. The primary reason for making these calculations was to obtain a theoretical indication of the effect of changes in the various derivatives on the initial response and resulting motions for use in explaining the flight-test results.

The effects on dynamic stability, control, and general flight behavior of artificially varying the derivatives are discussed independently for each derivative. Results are presented for a wide range of values (both positive and negative) for each derivative; however, since damping of the lateral oscillation is the primary function of any artificial-stabilization system, only variations of the derivatives in the direction which produces improvement in oscillatory stability are discussed in detail.

The experimental results, based on flight ratings for oscillatory stability and general flight behavior, are summarized in figure 18. In this summary a comparison is made of the improvements in oscillatory stability and of the accompanying changes in general flight behavior obtained by varying the different derivatives.

The effects of each derivative on the total damping of the system are presented in figure 19. These results are presented in order to provide a better understanding of the effects of the different derivatives on oscillatory stability and general flight behavior.

A comparison of the calculated effects of the four derivatives is shown in figure 20 in order to show the relative effectiveness of each derivative in providing satisfactory oscillatory stability. For this comparison the period and damping factor have been scaled up so that the results can also be compared directly with the Air Force and Navy damping requirements (refs. 10 and 11). In scaling up these values the model was assumed to be a $\frac{1}{9}$-scale model of an airplane; therefore, the period of the model was multiplied by 3 and the damping factor was divided by 3.

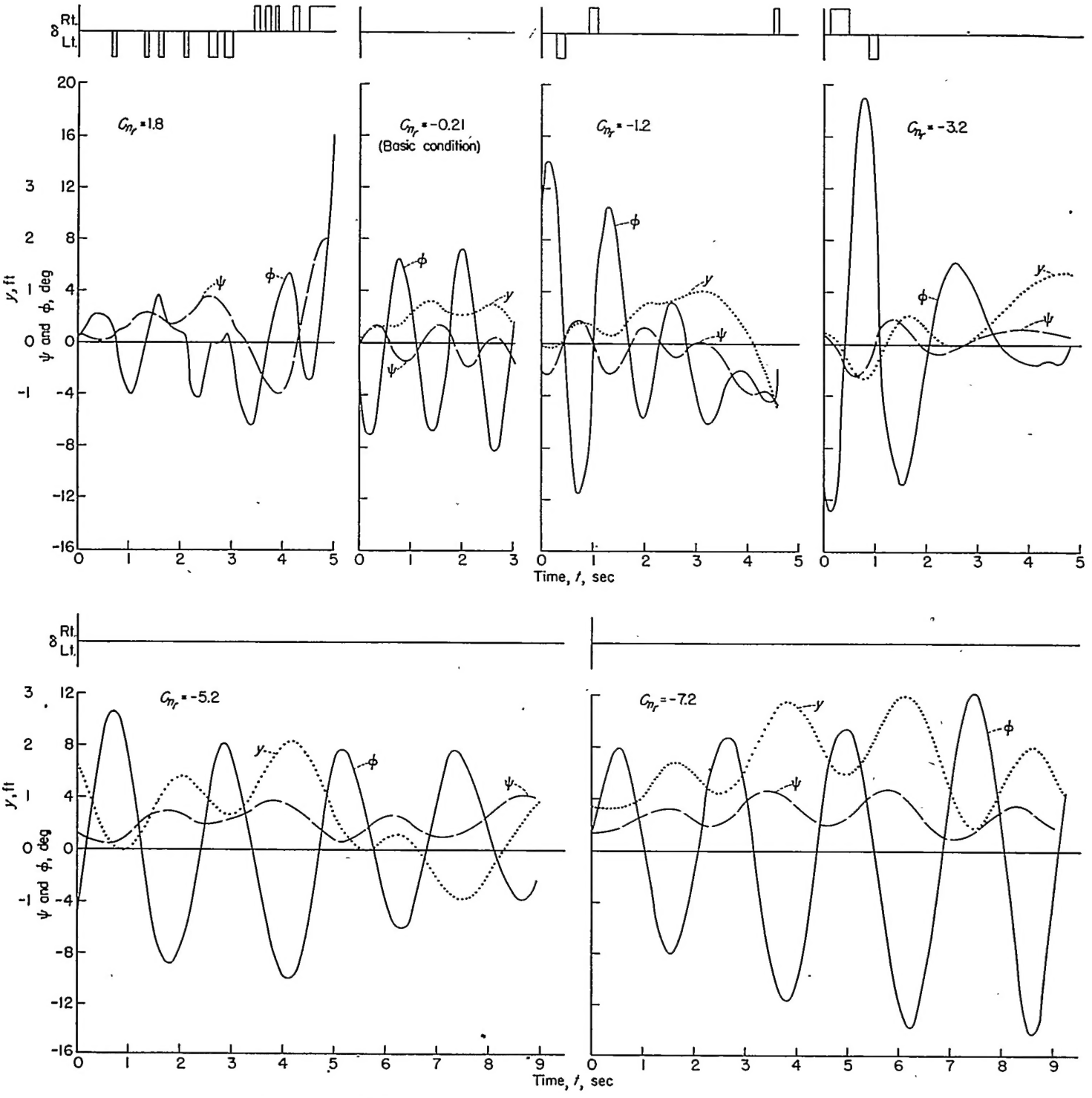

FIGURE 6.—Flight records of the lateral motions for various values of C_{n_r}.

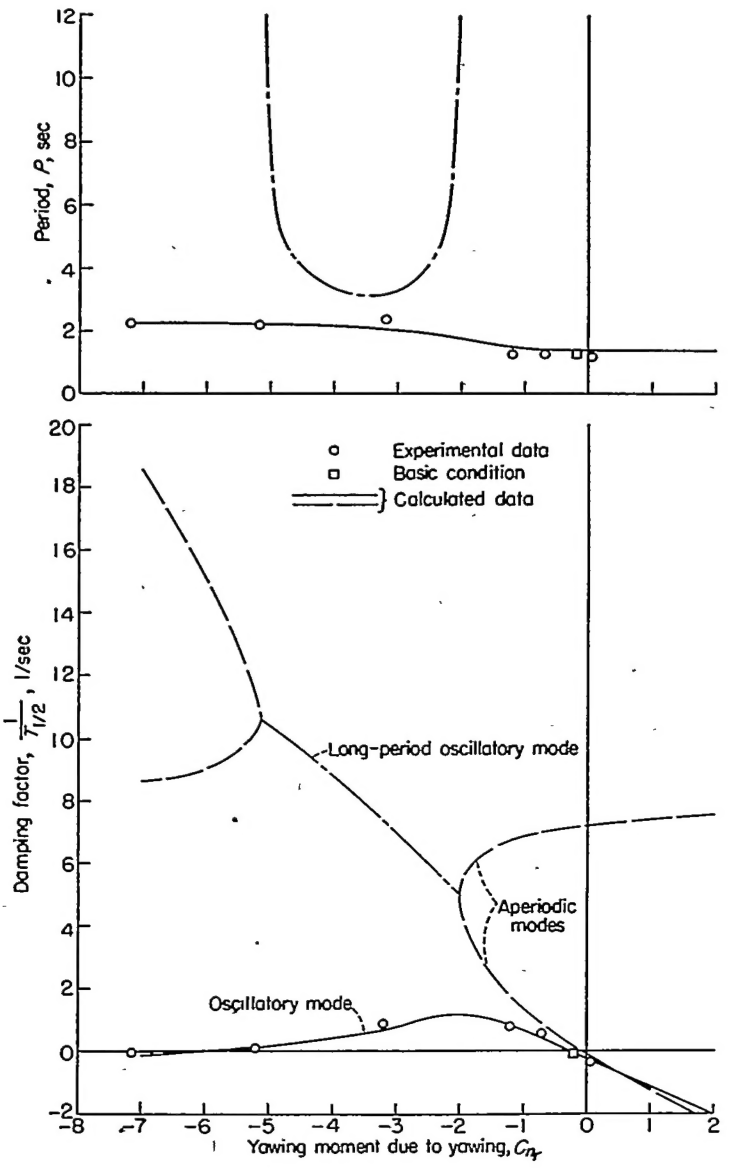

FIGURE 7.—Calculated effect of C_{n_r} on stability and comparison with experimental data.

EFFECT OF YAWING MOMENT DUE TO YAWING C_{n_r}

As C_{n_r} was increased in the negative direction, the damping of the lateral oscillation increased up to an optimum value and then decreased while the apparent spiral stability continued to improve. In this range the lateral control was good, and no apparent loss of maneuverability occurred with increasing C_{n_r}. The best general flight behavior was obtained with a value of C_{n_r} slightly greater than that which produced the greatest damping of the oscillation. A detailed discussion of the changes in dynamic stability, control, and general flight behavior is given in the following sections.

Dynamic stability.—In the basic condition ($C_{n_r}=-0.21$), the model had neutral oscillatory stability. The flight records of figure 6 indicate that moderate increases in the value of C_{n_r} in the negative direction caused a marked improvement in damping of the short-period lateral oscillation. Further negative increases in the value of C_{n_r} caused a reduction in damping of the oscillation; in fact, oscillatory instability was obtained with a value of C_{n_r} of −7.2. It appeared to the pilot that the best damping of the oscillation was obtained with values of C_{n_r} between −1 and −3.

When C_{n_r} was varied in the positive direction from the basic condition, the lateral oscillation became unstable. This instability increased until, at a value of C_{n_r} of 1.8, the model became so unstable that sustained flight was impossible. Neither the period nor the time for the oscillation to double amplitude could be estimated from the flight-test results in this range of C_{n_r} because the model could not be allowed to fly uncontrolled for more than a second or two at a time.

The comparison of the calculated and experimental values of period and damping of the lateral oscillation shown in figure 7 indicates good agreement for the various values of C_{n_r} covered in the tests. These results indicate that maximum damping of the oscillation was obtained with a value of C_{n_r} of about −2.0. For this value of C_{n_r}, the lateral oscillation damped to one-half amplitude in about 0.9 second. These results also show that the period of the oscillation increased from about 1.4 seconds to about 2.2 seconds as C_{n_r} was varied from −0.21 to −7.2.

For the higher negative values of C_{n_r} (−3.2 to −7.2), the flight tests indicated that the lateral motion of the model progressively changed from the normal Dutch roll oscillation to a pendulum type of oscillation that consisted mainly of roll and sidewise displacement. The time histories of figure 6 show that at a value of C_{n_r} of −7.2 the ratio of yaw to roll is approximately one-half the value obtained in the basic condition. This decrease in the ratio of yaw to roll is attributed to the fact that increasing the damping in yaw causes partial restraint of the yawing motions. This change in the nature of the lateral oscillation is also shown in the calculated motions in figure 8.

During the flight tests a change was also noted in the nonoscillatory dynamic lateral stability of the model as C_{n_r} was varied. Although the damping of the aperiodic modes of motion could not be measured from the flight-test records, the pilot was aware of increasingly better apparent spiral stability as C_{n_r} was increased negatively since the model would fly for long periods of time with controls fixed despite the natural gustiness of the air flow. This increase in apparent spiral stability is shown by the time histories (fig. 6) which indicate that it was possible to obtain longer uncontrolled flight records as C_{n_r} was increased negatively despite the lightly damped or unstable oscillations at the higher negative values of C_{n_r}. Since the pilot considered this flight characteristic desirable, the best spiral-stability ratings were obtained with the higher negative values of C_{n_r}.

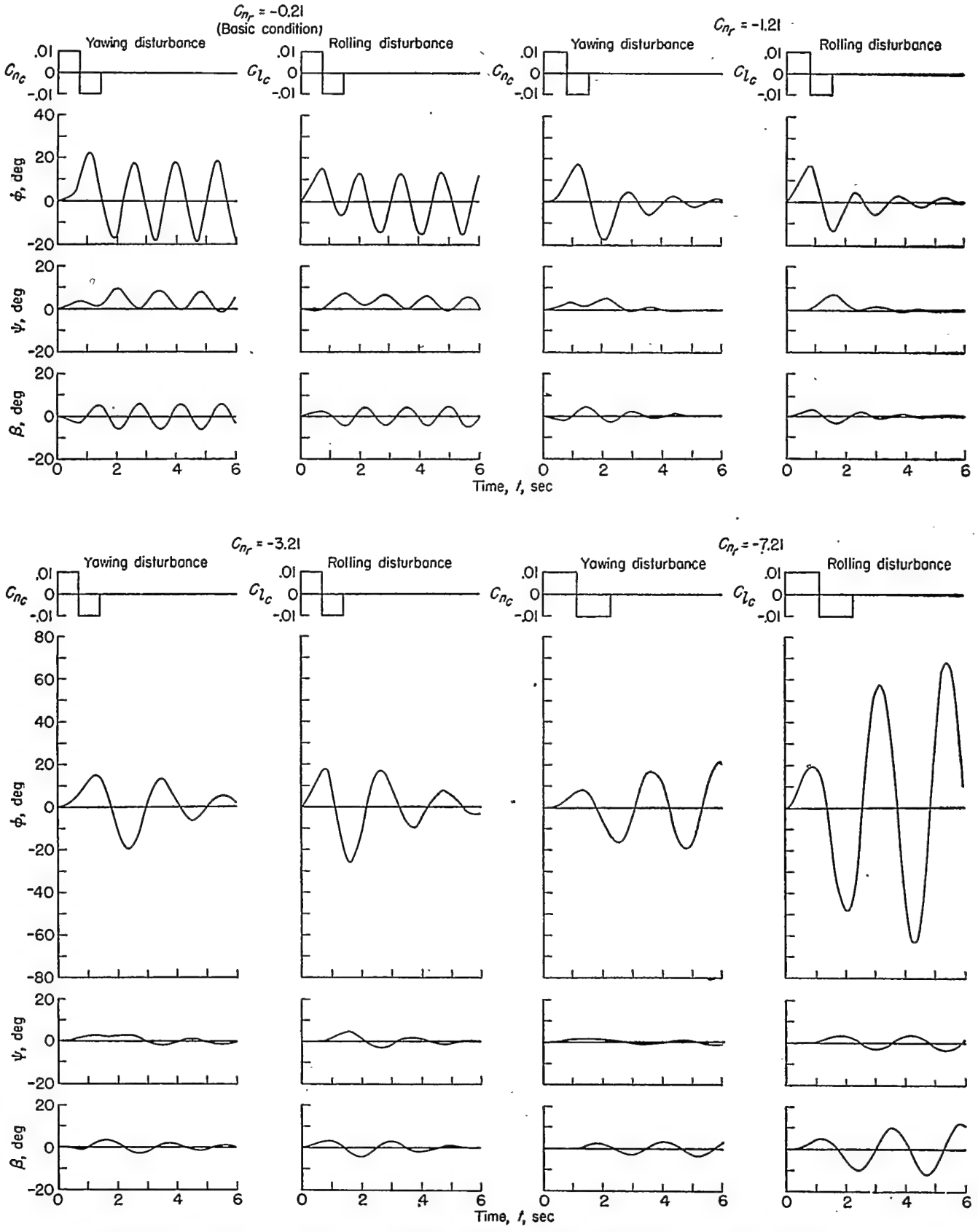

FIGURE 8.—Calculated response of model to yawing or rolling disturbance for various values of C_{n_r}

The calculated stability in the negative C_{n_r} range (fig. 7) indicates that the aperiodic modes merge to form a second oscillation for values of C_{n_r} between −2.0 and −5.2. This oscillation was so heavily damped that it was never observed in the model flights. The constantly increasing apparent spiral stability observed in the flight tests as C_{n_r} was varied in the negative direction appears to correspond to the increasing stability of first the spiral mode and then the long-period oscillation.

Control.—The lateral control characteristics are presented in table II in the form of ratings based on the pilot's opinion of the controllability and maneuverability of the model for various values of C_{n_r}.

It may be seen from this table that as C_{n_r} was varied in the negative direction the controllability improved. In the basic condition (case 7), despite the undamped oscillation, the model could be flown with only occasional corrective control deflections to keep the model in the center of the test section. As C_{n_r} was increased in the negative direction, the model required progressively less control and with the higher values of C_{n_r} would fly uncontrolled for relatively long periods of time. (See fig. 6.) The best lateral control of the model was obtained with a value of C_{n_r} of −3.2, when the lateral motion of the model following a disturbance would completely die out before any corrective control was required. When C_{n_r} was varied in the positive direction, the lateral control characteristics became worse. The model was barely controllable with the most positive value of C_{n_r} tested (case 9) since the unstable oscillatory motion and the unstable spiral mode necessitated constant corrective control deflections to prevent the model from crashing.

In the opinion of the pilot the model had adequate maneuverability throughout the range of C_{n_r} tested in that the model could be maneuvered to any desired position in the tunnel quickly and easily. In fact, had the model not been easily maneuverable, flight with positive values of C_{n_r} might have been impossible because of both oscillatory and spiral instability. In the negative range of C_{n_r}, it was not possible to note the decreased maneuverability or increased stiffness in making turns which has been experienced with some airplanes equipped with yaw dampers (ref. 12) since steady turning maneuvers cannot be made in the Langley free-flight tunnel because of restrictions imposed by the size of the test section.

General flight behavior.—The general flight behavior of the model in the basic condition (case 7) was not satisfactory because of the undamped lateral oscillation. As C_{n_r} was increased negatively, the general flight behavior of the model improved as a result of both the increased damping of the oscillation and the improved spiral stability. The best general flight behavior was obtained with a value of C_{n_r} of −3.2 (case 3). Although this value of C_{n_r} produced less damping of the oscillation than the maximum obtained with C_{n_r} equal to −2.2, the pilot felt that the overall flight characteristics obtained were a little better because of the better spiral stability and because the model appeared to be somewhat easier to control. As C_{n_r} was further increased negatively, the progressive decrease in oscillatory stability and the appearance of the objectionable pendulum type of oscillation resulted in poorer general flight behavior. With values of C_{n_r} greater than −5.2 (cases 1 and 2), the overall flight characteristics of the model were unsatisfactory because of the lightly damped or unstable oscillation.

When C_{n_r} was increased in the positive direction from the basic condition (cases 8 and 9), the general flight behavior became very poor because of both the oscillatory and spiral instability.

EFFECT OF ROLLING MOMENT DUE TO ROLLING C_{l_p}

Small negative increases in the value of C_{l_p} caused the damping of the lateral oscillation to improve rapidly, but further negative increases in C_{l_p} resulted in no further improvement in the oscillatory stability. Most of the damping added to the system by these further increases in C_{l_p} was absorbed by the aperiodic rolling mode so that the model appeared to be very stiff in roll. Although this flight characteristic caused the model to have very poor maneuverability in roll, the model was very easy to control in a wings-level attitude. The general flight behavior was considered satisfactory only for small negative values of C_{l_p}.

Dynamic stability.—The results for the damping of the lateral oscillation indicate that as C_{l_p} was increased in the negative direction from the basic value of −0.32 the damping rapidly improved for values of C_{l_p} up to about −0.6 (case 13, table II). As C_{l_p} was further increased, the oscillation could not be initiated because the rolling mode was so heavily damped that the model was essentially restrained from rolling (cases 10 and 11). The time histories in figure 9 show this change in the nature of the motion. In the high negative range of C_{l_p} (−1.0 to −7.0), some flights were made in which the initiation of oscillations by rudder deflection was attempted, but these attempts to obtain oscillations were not successful because the model sideslipped into the tunnel wall before enough cycles of the oscillation were obtained to permit measurement of the damping. With a value of C_{l_p} of −0.8, the oscillation damped to one-half amplitude in about 1.4 seconds.

The flight records show that increasing C_{l_p} in the positive direction caused the lateral oscillation of the model to become unstable. This instability increased very rapidly and, with a rather small positive value of C_{l_p} (0.1), sustained flight was impossible.

A comparison of the experimental and calculated values of period and damping of the model is presented in figure 10. These results show that the experimental values of period and damping are in fairly good agreement with the calculated values for the limited range of negative C_{l_p} where the period and damping could be measured. The calculations show that

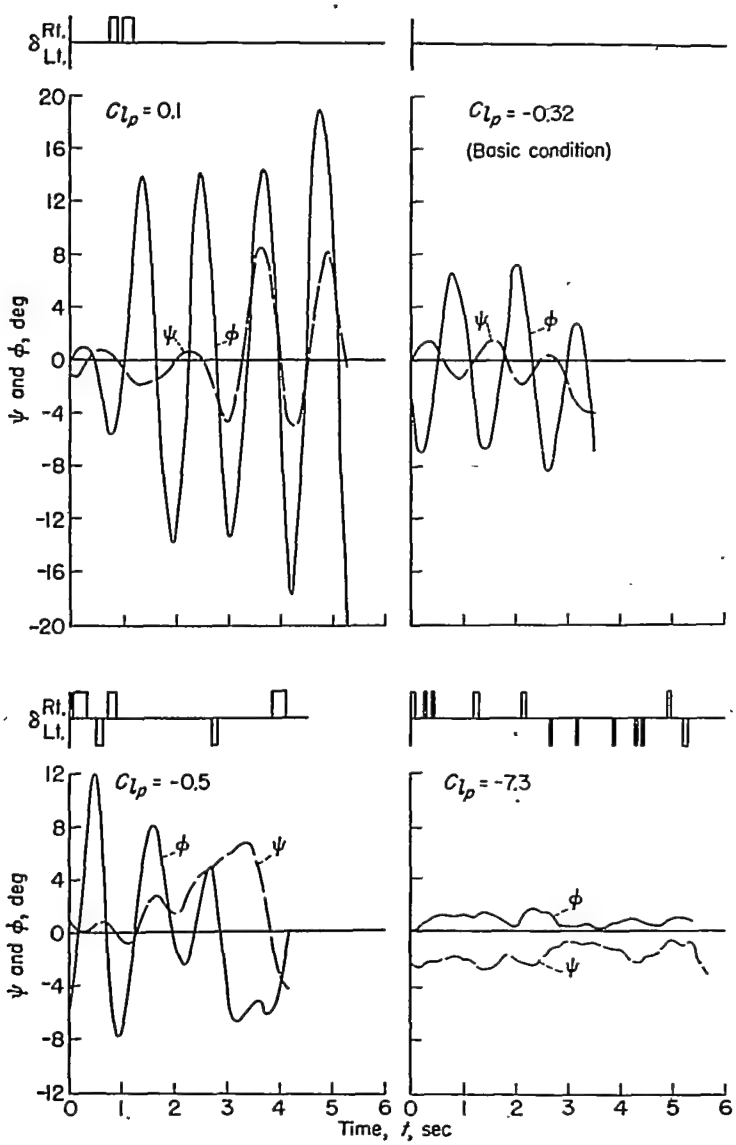

FIGURE 9.—Flight records of the lateral motions for various values of C_{l_p}.

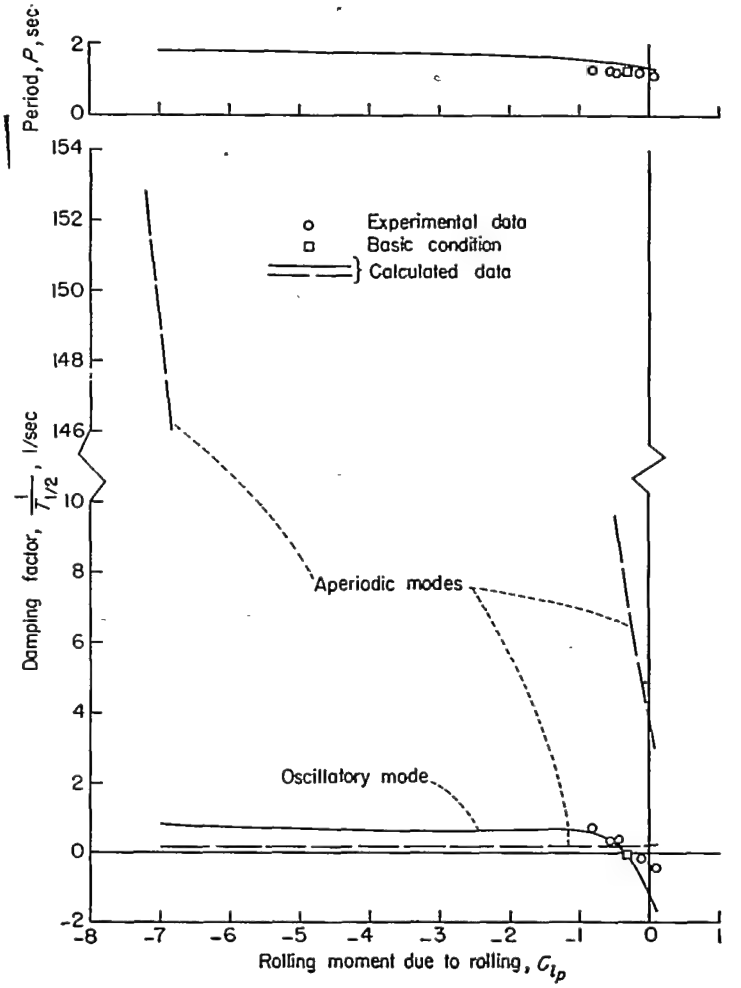

FIGURE 10.—Calculated effect of C_{l_p} on stability and comparison with experimental data.

for negative values of C_{l_p} greater than −0.9 damping of the oscillation did not increase further. Although the calculations correctly predicted the existence of an unstable oscillation in the positive C_{l_p} region, the oscillatory instability $\left(\frac{1}{T_{1/2}}=-0.50\right)$ determined from the flight-test results for $C_{l_p}=0.10$ was not so severe as that predicted by the calculations in which time lag was assumed to be negligible $\left(\frac{1}{T_{1/2}}=-1.70\right)$. Additional calculations showed that for this same value of C_{l_p} a value of $1/T_{1/2}$ of zero (neutral stability) would be obtained with a time lag of about 0.10 second. By interpolation the calculated results can be assumed to indicate that the actual time lag of 0.05 second known to exist in the stabilization device would result in a value of $1/T_{1/2}$ of about −0.85, which is in better agreement with the experimentally determined value of −0.50. The discrepancy between the measured and calculated values of damping shown in figure 10 may therefore be attributed at least partly to the effect of time lag in the stabilization system.

The most significant change in the dynamic stability of the model as C_{l_p} was varied in the negative direction was the very rapid increase in stability of the rolling mode. In the flight tests this increase in rolling stability was evidenced by an increase in the stiffness in roll as C_{l_p} was increased negatively. With very large negative values of C_{l_p} the model was essentially restrained from rolling. When C_{l_p} was increased in the positive direction from the basic condition, the model became overly sensitive to aileron control; this sensitivity indicates that the stability of the rolling mode decreased. No noticeable change in damping of the spiral mode of motion occurred throughout the C_{l_p} range covered in the tests.

The tendency toward restraint in roll experienced in the flight tests is indicated in the calculated results (fig. 10) which show that one of the aperiodic modes (the rolling mode) became increasingly stable as C_{l_p} was increased negatively. The calculated response for various values of C_{l_p} presented in figure 11 shows the reduction in amplitude of the rolling motion as C_{l_p} was increased negatively from the basic condition.

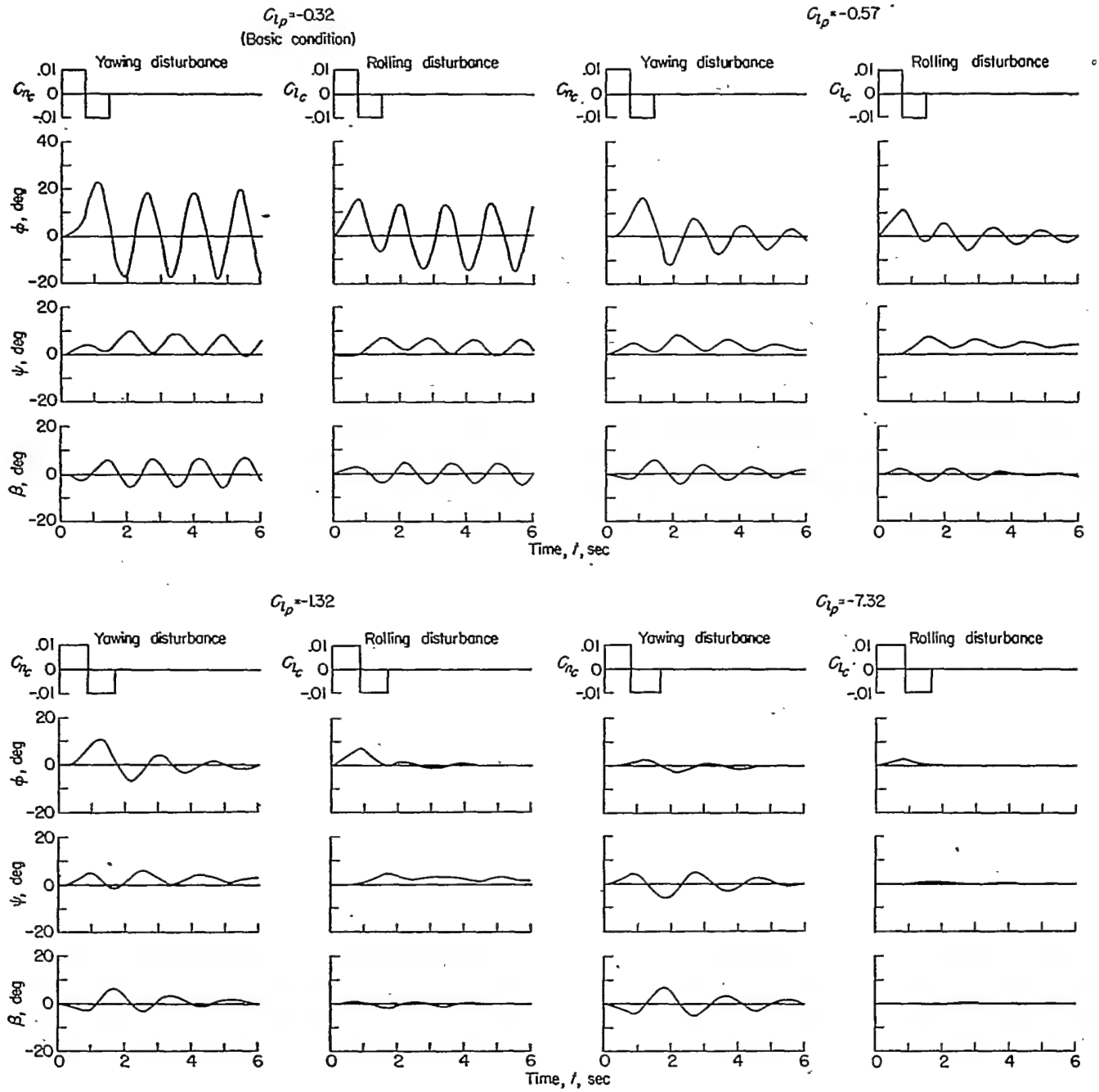

FIGURE 11.—Calculated response of model to yawing or rolling disturbance for various values of C_{l_p}.

The flight records (fig. 9) show that the negative damping in roll (positive C_{l_p}) caused the model to have an unstable oscillation rather than an aperiodic divergence or roll-off. Apparently the reason for this result is the fact that the rolling mode was still stable for the highest positive value of C_{l_p} covered in the tests. (See fig. 10.)

Control.—The lateral-control ratings presented in table II indicate that increasing C_{l_p} in the negative direction caused the model to have good controllability but poor maneuverability (cases 10 to 14). The tendency toward restraint in roll imposed by high negative values of C_{l_p}, although undesirable for maneuverability, caused the model to be very steady and to require very little corrective control when flown in a steady wings-level attitude. The best lateral control characteristics were obtained with a value of C_{l_p} of about −0.6, where the oscillation required little control and the stiffness in roll was not excessive. The overall lateral control characteristics of the model with very large negative values of C_{l_p} were considered unsatisfactory because of the reduced maneuverability.

The adverse effect of high negative values of C_{l_p} on maneuverability might be eliminated without sacrificing the desirable steadiness in wings-level flight by utilizing a control system similar to that suggested in reference 12 for an airplane equipped with a yaw damper. In performing maneuvers with an airplane equipped with one form of such a

control system, deflection of the control stick would not directly deflect the ailerons but would modify the signal from the rate-sensing device to the servoactuator such that the aileron would be deflected in the manner required to perform the desired maneuver. The stiffness in roll apparent to the pilot could thereby be greatly reduced. In some preliminary tests with another model, results with this type of control system have been very satisfactory.

When C_{l_p} was varied in the positive direction from the basic condition (from case 7 to case 15), constant corrective control was required because of the unstable oscillation, but the model was highly maneuverable in roll. This increase in maneuverability was attributed to the reduced damping of the rolling mode. (See fig. 10.)

General flight behavior.—The two important factors affecting the overall flight characteristics of the model when C_{l_p} was varied were the damping of the oscillation and the overdamping of the rolling mode. The best general flight behavior was obtained with a value of C_{l_p} of −0.8 (case 12). For this condition, the oscillation damped to one-half amplitude in about 1.4 seconds and the tendency toward restraint in roll was not considered too objectionable, although the model did have less rolling maneuverability than is normally desired. Steady wings-level flights with this value of C_{l_p} were very smooth and the model required very little corrective control.

For values of C_{l_p} between −0.5 and 0.1 (cases 14, 7, and 15), the general flight behavior was poor because of unsatisfactory damping of the lateral oscillation. With values of C_{l_p} between −0.8 and −7.3 (cases 10 to 12), the general flight behavior was considered unsatisfactory because the rolling mode was so heavily damped that the rolling maneuverability of the model was impaired.

EFFECT OF ROLLING MOMENT DUE TO YAWING C_{l_r}

Increasing C_{l_r} in the positive direction improved the damping of the lateral oscillation but caused the model to become very spirally unstable. No flight condition in which C_{l_r} was varied was considered appreciably better than the basic flight condition.

Dynamic stability.—The flight tests show that the damping of the lateral oscillation improved very slightly when C_{l_r} was increased from the basic value of 0.13 to a value of 0.3 (fig. 12 and table II), but the model became more difficult to fly despite this increase in damping. With values of C_{l_r} greater than 0.3, attempts to measure the damping of the oscillation were not successful because almost continuous corrective control was required to keep the model from diverging into the tunnel walls. In this range of C_{l_r}, however, it was apparent to the pilot that the damping of the oscillation was increasing with increasing C_{l_r}. (See cases 19 and 20, table II.)

When C_{l_r} was varied in the negative direction from the basic condition, oscillatory instability was obtained, but even with the highest negative value of C_{l_r} covered in the tests (−2.9), this instability was not great enough to make

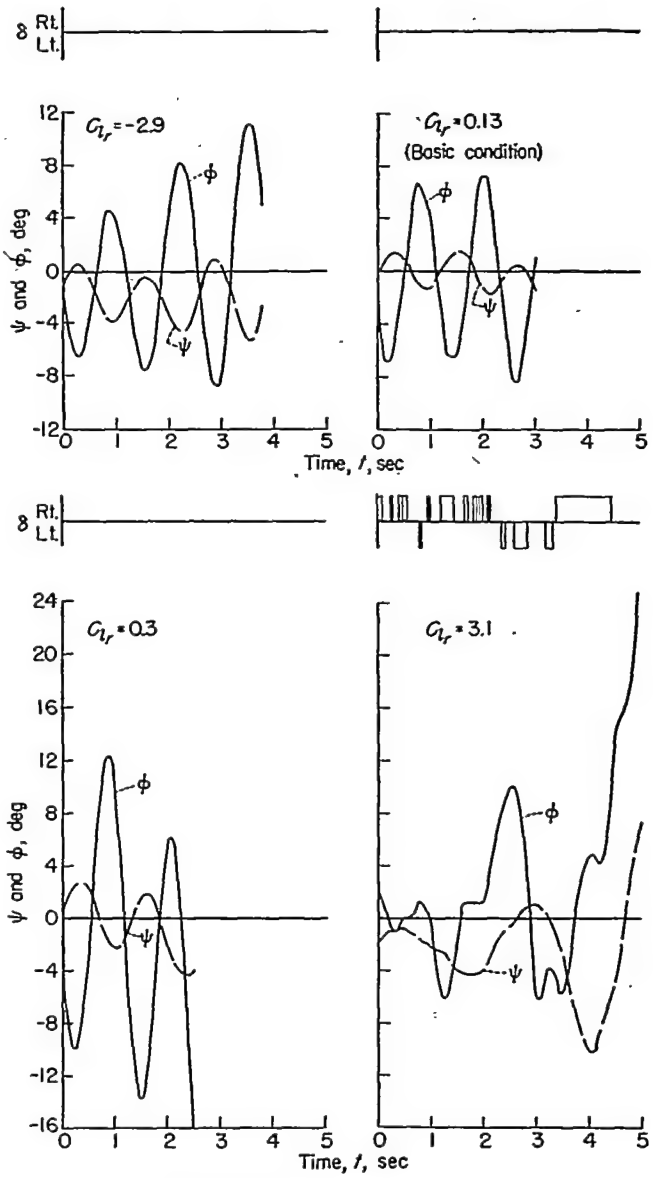

FIGURE 12.—Flight records of the lateral motions for various values of C_{l_r}.

the model unflyable. For this value of C_{l_r}, the oscillation doubled amplitude in about 3.0 seconds.

A comparison of the calculated and experimental values of period and damping as affected by changes in C_{l_r} is presented in figure 13. In the positive C_{l_r} range above 0.3, no quantitative data on the damping of the oscillation could be obtained, as previously mentioned. The data of figure 13 show that, for all values of C_{l_r} except those close to the basic value of 0.13, the calculated damping of the oscillation is in rather poor agreement with the experimental results. In the negative C_{l_r} range the instability of the oscillation was not nearly as severe as that predicted by the calculations in which time lag was neglected. For the value of C_{l_r} of −2.9, the measured value of $1/T_{1/2}$ was about −0.35, whereas that calculated with the assumption of zero time lag was approximately −2.50. In an effort to explain this large difference between the experimental and calculated results, additional calculations were made in

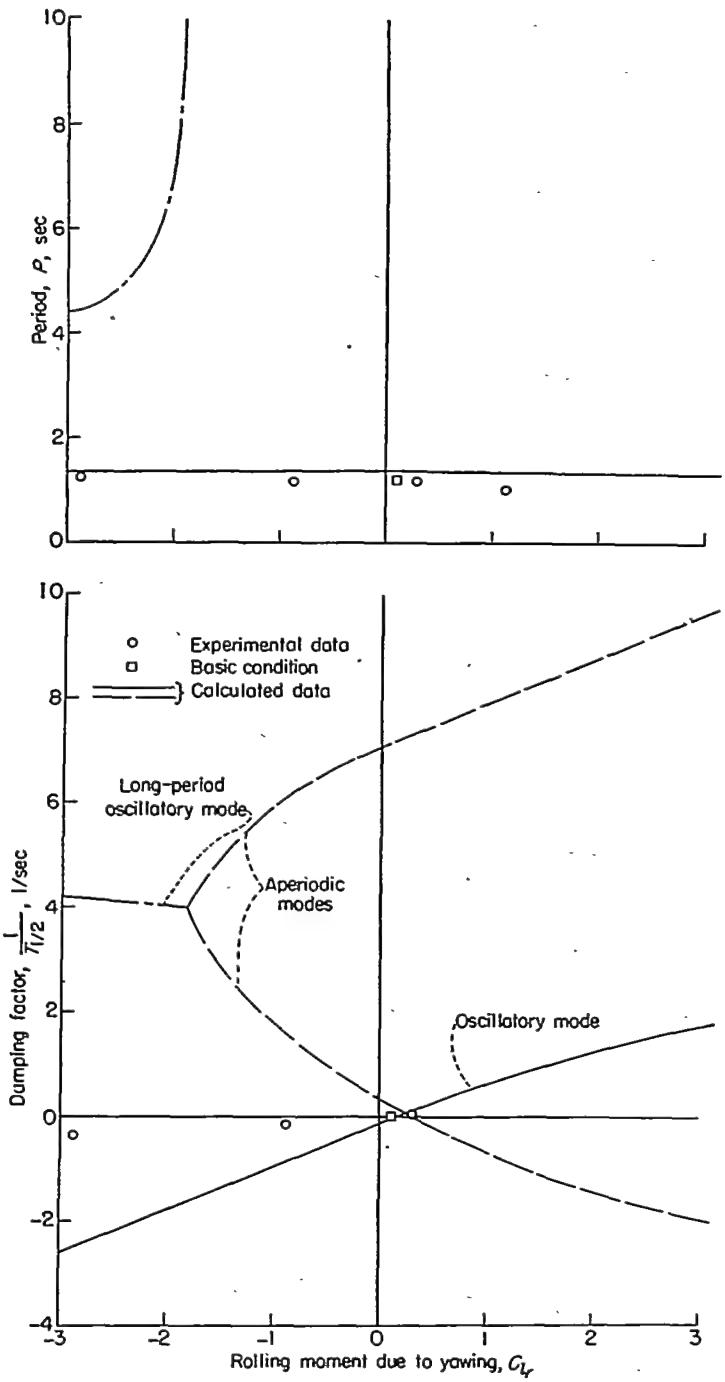

FIGURE 13.—Calculated effect of C_{l_r} on stability and comparison with experimental data.

which the constant time lag of 0.05 second was taken into account. The result of these calculations $\left(\frac{1}{T_{1/2}}=-1.32\right)$ was in closer agreement with the experimental value of $1/T_{1/2}$. The discrepancy between the measured and calculated values of damping shown in figure 13 may therefore be attributed at least partly to the effect of time lag in the stabilization device. The calculated period, which was relatively unaffected by time lag, is in fairly good agreement with the period determined from flight records for all values of C_{l_r} where oscillations could be obtained. These results indicate that almost no variation in period occurred throughout the range of C_{l_r}. The calculated response of the model for a value of C_{l_r} of 3.13 (fig. 14) illustrates the aperiodic divergence which made it impossible to obtain a quantitative measurement of damping in the flight tests for large positive values of C_{l_r}.

The most noticeable change in stability observed in the flight tests was the severe spiral divergence encountered with high positive values of C_{l_r}. Spiral instability occurred with a value of C_{l_r} of about 0.3 and became more severe as C_{l_r} was increased. With a value of C_{l_r} of 3.1 (case 20), this spiral instability was so great that most of the flights ended in crashes. This increase in spiral instability observed in the flight tests is predicted by the damping calculations of figure 13 and is illustrated by the calculated response to rolling and yawing disturbances in figure 14.

In the flight tests the spiral stability appeared to be improved as C_{l_r} was increased in the negative direction since the model would fly for long periods of time with controls fixed. This increase in spiral stability was also predicted by the calculations. (See fig. 13.) The long-period heavily damped oscillation, which the calculations show is formed from the merger of the spiral and rolling modes in the negative C_{l_r} range, was not apparent in the flight tests.

From these results the variation of the derivative C_{l_r} appears to offer very little hope for improving the overall lateral stability characteristics of an airplane. This derivative, however, may in some cases be used to redistribute the damping between the oscillatory and aperiodic modes if surplus damping of the aperiodic modes is initially present. Preliminary calculations have indicated that the damping of the oscillation obtained with C_{n_r} alone could be improved appreciably by utilizing C_{l_r} to redistribute part of the excess damping of the spiral mode to the oscillatory mode.

Control.—As C_{l_r} was varied in the positive direction, the model became more maneuverable but the controllability became worse. The increased maneuverability caused the model to be highly responsive to the slightest control deflection at the higher values of C_{l_r} so that the model became very difficult to control. Many of the flights with a value of C_{l_r} of 3.1 ended in crashes because the model was inadvertently overcontrolled; yet, reducing the control deflection did not seem advisable because at times large control deflections were required to recover from the rapid roll-off into a spiral. (See fig. 12.) In this case the model appeared to be highly maneuverable when the pilot rolled the model from an initial wings-level flight attitude; however, in the attempt to recover from a large angle of bank following such a roll-off, application of full opposite control did not produce immediate recovery. The maneuverability in this condition was therefore considered not entirely satisfactory. Because of the inability to establish a definite overall estimate of the maneuverability with positive values of C_{l_r}, no maneuverability ratings were assigned for these conditions in table II.

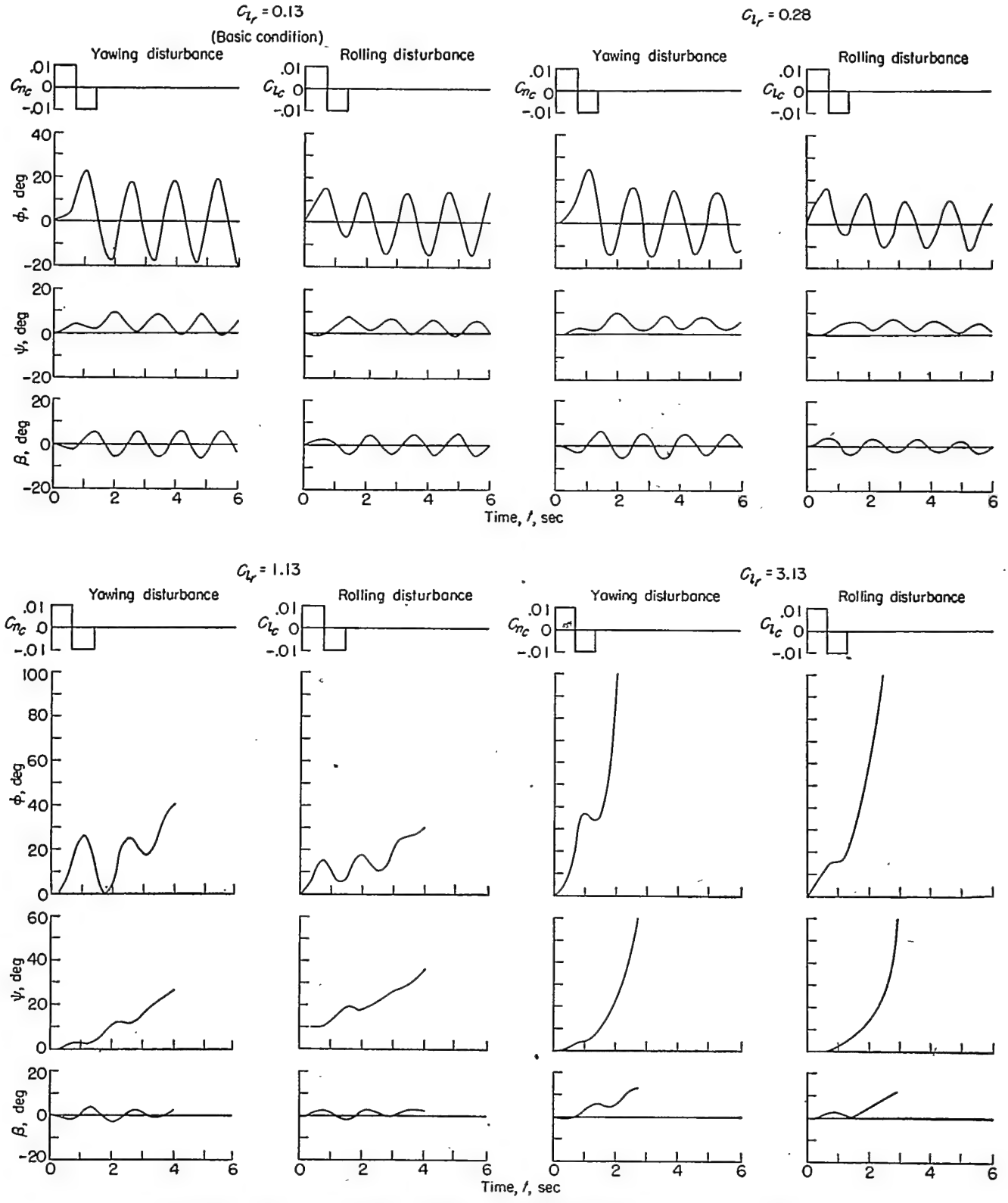

FIGURE 14.—Calculated response of model to yawing or rolling disturbance for various values of C_{l_r}.

When C_{l_r} was varied in the negative direction (cases 16 and 17), the controllability became worse because corrective control was required to prevent the unstable oscillation from building up to large amplitudes. Even at the highest negative value of C_{l_r} tested, however, the oscillatory instability was easily controlled. The maneuverability of the model was satisfactory in the negative range of C_{l_r} and was not appreciably different from that of the basic condition.

General flight behavior.—The only improvement in the general flight behavior that resulted from varying C_{l_r} was obtained with a very small positive increase (from 0.13 to 0.3), and this improvement was very slight. In this condition (case 18) the slight increase in oscillatory stability was considered more important to the general flight behavior than the decrease in controllability. With further positive increases in C_{l_r} (cases 19 and 20), the general flight behavior became worse despite the increase in oscillatory stability. Poor controllability and severe spiral instability, which more than offset the increased damping of the lateral oscillation, were the causes of this poor general flight behavior. As C_{l_r} was increased in the negative direction, the unstable oscillation caused the general flight behavior of the model to become worse.

These results indicate that very little improvement in overall flight behavior of an airplane can be obtained with a change in C_{l_r}, except, perhaps, in the case of an airplane with a substantial amount of aperiodic stability in the basic condition.

EFFECT OF YAWING MOMENT DUE TO ROLLING C_{n_p}

Increasing the value of C_{n_p} in the positive direction caused a very rapid improvement in damping of the lateral oscillation, but this improvement in damping was obtained at the expense of the normally well-damped rolling mode. The decrease in the stability of the rolling mode caused the controllability and hence the general flight behavior of the model to become progressively worse.

Dynamic stability.—The results of flight tests indicated that a small positive increase in the value of C_{n_p} caused a large improvement in damping of the lateral oscillation. The time histories of figure 15 show that as the value of C_{n_p} was increased from −0.07 (basic condition) to 0.3 the neutrally stable oscillation became well-damped. For this value of C_{n_p} the oscillation damped to one-half amplitude in about 0.8 second. With further increases in the value of C_{n_p} to 0.9, quantitative values for damping of the oscillation could not be measured from the flight records because the poor lateral flight behavior of the model required almost constant corrective control. In this range of C_{n_p} (cases 23 to 25), however, it was apparent to the pilot that the damping of the oscillation was increasing with increasing C_{n_p}.

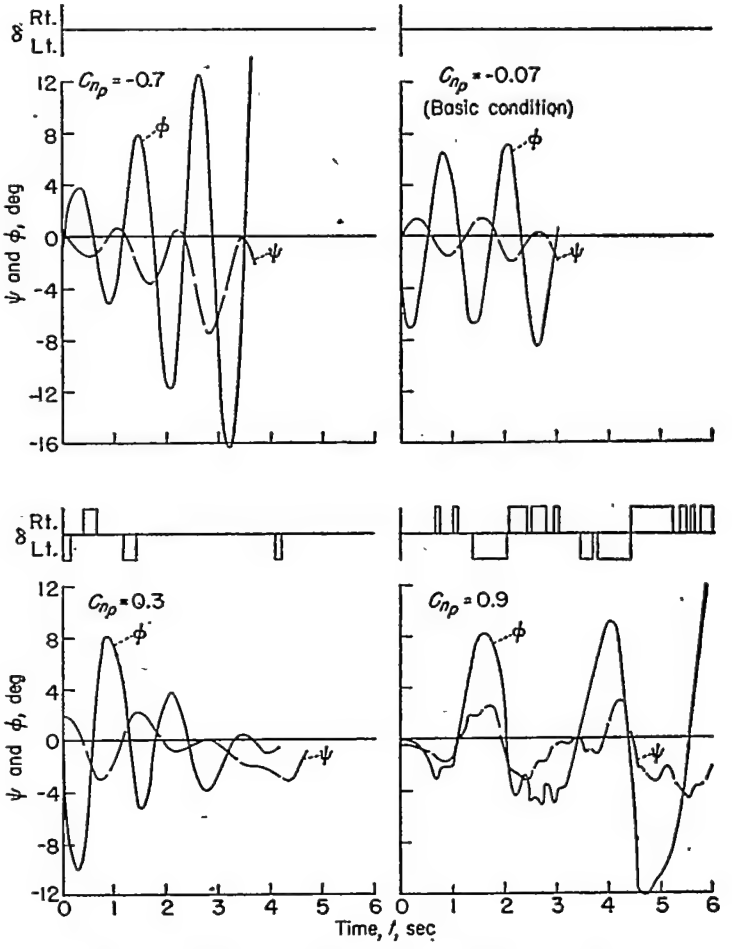

FIGURE 15.—Flight records of the lateral motions for various values of C_{n_p}.

(See table II.) Sustained flight was impossible with values of C_{n_p} greater than 0.9.

The results of flight tests indicated that as C_{n_p} was varied in the negative direction from the basic condition the lateral oscillation became unstable. Because of this increase in oscillatory instability, the negative range of C_{n_p} that could be experimentally investigated was very limited. With negative values of C_{n_p} larger than −0.7, the model was unflyable.

In the comparison of the experimental and calculated oscillatory stability of the model for various values of C_{n_p} (fig. 16), the theory is seen to be in fairly good agreement with the experimental results for damping of the oscillation. The increase in period for small positive values of C_{n_p} predicted by the calculations, however, was not observed in the flight tests. The calculations predict a continued increase in damping of the short-period oscillation for positive values of C_{n_p} larger than the maximum value tested (0.9) for which flights could be made. The calculated response of the model (fig. 17) for the value of C_{n_p} of 0.88 shows the aperiodic divergence

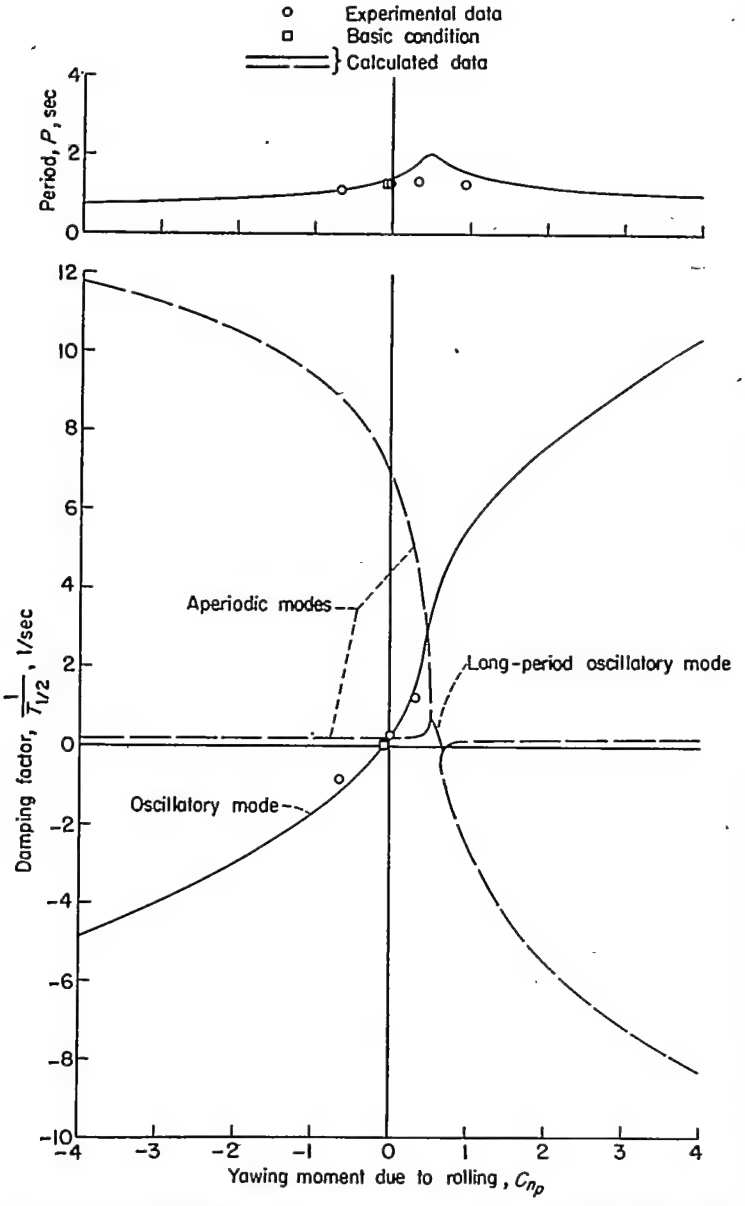

FIGURE 16.—Calculated effect of C_{n_p} on stability and comparison with experimental data.

which made a quantitative measurement of damping impossible to obtain in the flight tests for this case. In the negative range of C_{n_p} the calculations verify the highly unstable oscillation observed in the flight tests.

The improvement in oscillatory stability with positive values of C_{n_p} was accompanied by a decrease in the stability of the aperiodic phases of the motion. Flight tests were limited in this range by a type of instability which bore a close resemblance to the spiral instability observed in the flight tests with positive C_{l_r}. The model became very touchy to fly as C_{n_p} was increased up to 0.4 and became extremely difficult to control for values of C_{n_p} greater than 0.4. Because of this instability sustained flight was impossible for values of C_{n_p} greater than 0.9. As the value of C_{n_p} was varied through this range (−0.07 to 0.9), the pilot complained of an increasingly strong tendency of the model to go into a tight turn in response to normal aileron control. To the pilot this tendency appeared to be a severe case of spiral instability. The results of calculations, however, show that the stability of the spiral mode remained unchanged up to a value of C_{n_p} of 0.5, whereas the stability of the rolling mode decreased rapidly. (See fig. 16.) A decrease in stability of the rolling mode therefore might sometimes be mistaken for spiral instability.

The calculated results in figure 16 show that, although the rolling mode remained stable up to the point of its merger with the spiral mode at a value of C_{n_p} of about 0.55, it was considerably less damped than in any other flight condition experienced in these tests. At the value of C_{n_p} of 0.55, the two aperiodic modes merged to form a long-period oscillation which became unstable at a value of C_{n_p} of about 0.65. This oscillation was not observed in the flight tests because of its extremely long period of over 40 seconds. Immediately after it became unstable, the long-period oscillation broke up to form two new aperiodic modes, one of which became increasingly unstable as C_{n_p} was increased further.

The results of these tests and calculations indicate that the derivative C_{n_p} might possibly be useful for redistributing the natural damping of an airplane in cases where the airplane has more than adequate damping of the rolling mode. The results of reference 2 indicate that the use of C_{n_p} in combination with C_{l_p} will provide an increase in oscillatory stability without a loss in rolling stability since, as previously discussed, the use of the derivative C_{l_p} alone causes a large increase in the stability of the rolling mode. Use of C_{n_p} alone, however, obviously is limited to values less than those which would cause the undesirable aperiodic motions experienced in these tests.

Control.—Despite the increased damping of the lateral oscillation as C_{n_p} was increased from 0.3 to 0.4 (cases 23 and 24), the controllability of the model became worse as a result of the increase in apparent spiral instability. With small positive increases in the value of C_{n_p} ,the maneuverability of the model improved, and with the highest positive value of C_{n_p} covered in the tests (0.9, case 25), the model appeared to be highly maneuverable when the pilot rolled the model from an initial wings-level attitude. As in the case of high positive C_{l_r}, in an attempt to recover from a large angle of bank following such a roll-off, application of full opposite control did not produce immediate recovery. The maneuverability in this case was therefore considered not entirely satisfactory. Because of the inability to establish an overall estimate of the maneuverability with positive values of C_{n_p}, no maneuverability ratings were made for these conditions in table II.

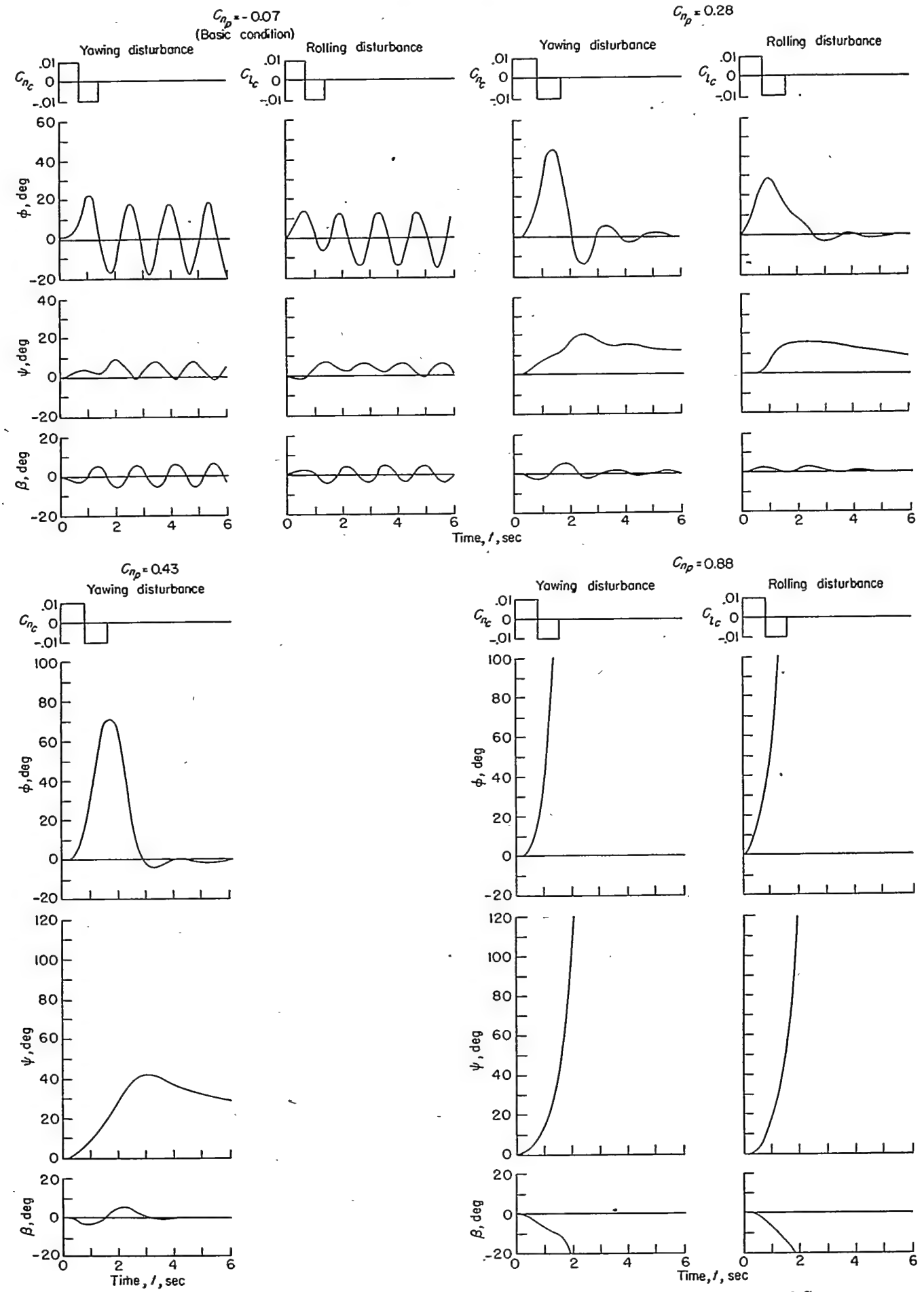

FIGURE 17.—Calculated response of model to yawing or rolling disturbance for various values of C_{n_p}.

When C_{n_p} was varied in the negative direction the controllability became poor because constant corrective control was required to prevent the unstable oscillation from building up to a large amplitude. The model was uncontrollable with values of C_{n_p} more negative than -0.7. There was no appreciable change in the maneuverability of the model with negative increases in C_{n_p}.

General flight behavior.—The increased damping of the oscillation obtained with the small positive values of C_{n_p} provided an improvement in the general flight behavior despite the decrease in apparent spiral stability. The pilot felt that, with the small positive values of C_{n_p}, the slight tendency toward spiral instability (which, in reality, was decreased damping of the rolling mode) was not highly objectionable because only small amounts of corrective control were required. With further positive increases in the value of C_{n_p}, however, the unstable aperiodic tendency became so severe that the general flight behavior was unsatisfactory even though the oscillatory stability continued to improve. When C_{n_p} was varied in the negative direction from the basic condition, the general flight behavior became worse because of the unstable oscillation.

COMPARISON OF EFFECTS OF THE ROTARY DERIVATIVES

Dynamic stability and general flight behavior.—The summary of results presented in figure 18 provides an indication of the relative merit of changes in the various derivatives. This summary, which is based on the flight ratings for oscillatory stability and general flight behavior (table II), compares the improvement in oscillatory stability and the accompanying changes in general flight behavior obtained by varying the different derivatives.

Use of C_{n_r} appears to produce the most satisfactory results since it provided the greatest amount of damping of the oscillation before introducing adverse flight characteristics. Although the results of figure 18 show that C_{l_p} produced approximately the same maximum damping of the oscillation as C_{n_r}, the poor maneuverability caused by the stiffness in roll which resulted from negative increases in C_{l_p} prevented good flight behavior from being obtained. In fact, for values of the derivatives of about -2 or -3 where the damping was essentially the same for the two derivatives, the flight behavior for C_{l_p} was considered poor whereas that for C_{n_r} was good.

Although the two cross derivatives C_{l_r} and C_{n_p} actually produced a greater improvement in the damping of the oscillation than the two damping derivatives C_{n_r} and C_{l_p}, they provided less improvement in general flight behavior. In fact, because of the severe apparent spiral instability produced by increases in these derivatives, satisfactory general flight behavior could not be obtained for any condition in which C_{l_r} was varied, and only barely satisfactory general flight behavior could be obtained with C_{n_p}.

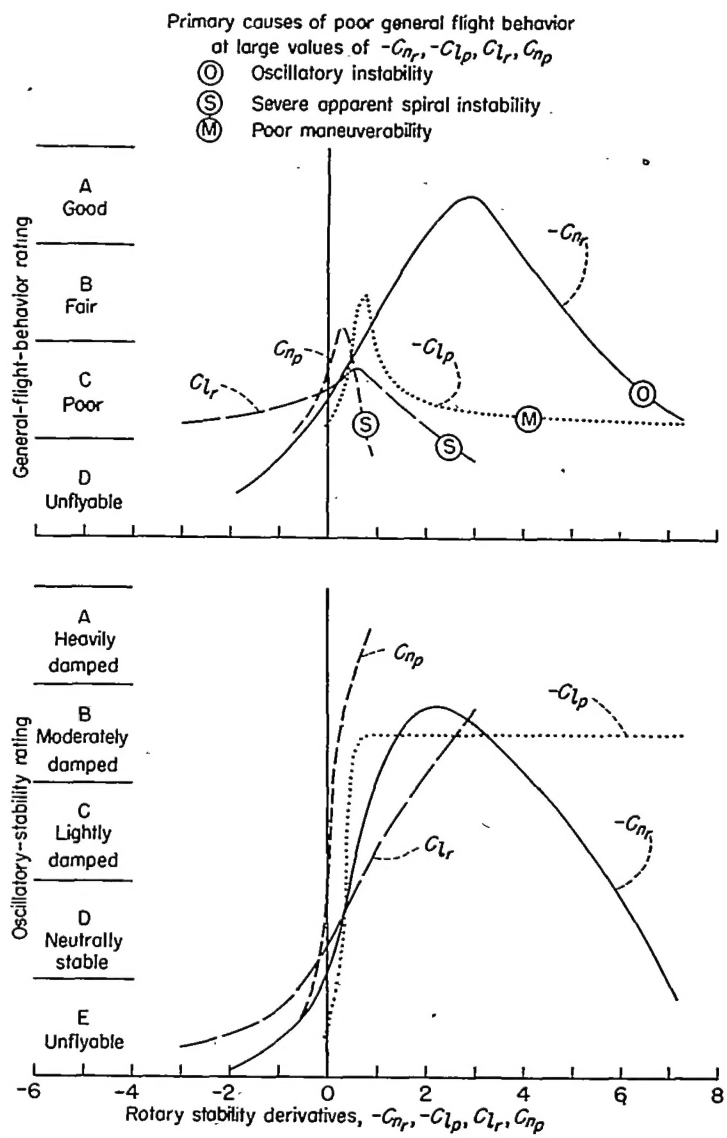

FIGURE 18.—Effect of variation in rotary derivatives on general flight behavior and oscillatory stability. (Data from table II.)

Amount and distribution of the damping of the system.—For a better understanding of the effects of the derivatives on the oscillatory stability and general flight behavior, both the changes in total damping of the system and the redistribution of this damping between the various lateral modes must be considered. The results presented in figure 19 show the way each derivative affects the total damping of the system. In this comparison the damping is expressed in terms of the ratio B/A where A and B are coefficients of the first two terms of the lateral-stability quartic equation. This ratio is proportional to the total damping. (See refs. 1 and 2.)

These results show that changes in any of the four derivatives can cause increases in the total damping. The greatest increase in damping per unit change in a derivative was obtained with negative increases in the value of C_{l_p}. Increasing the value of C_{n_r} negatively was about one-seventh

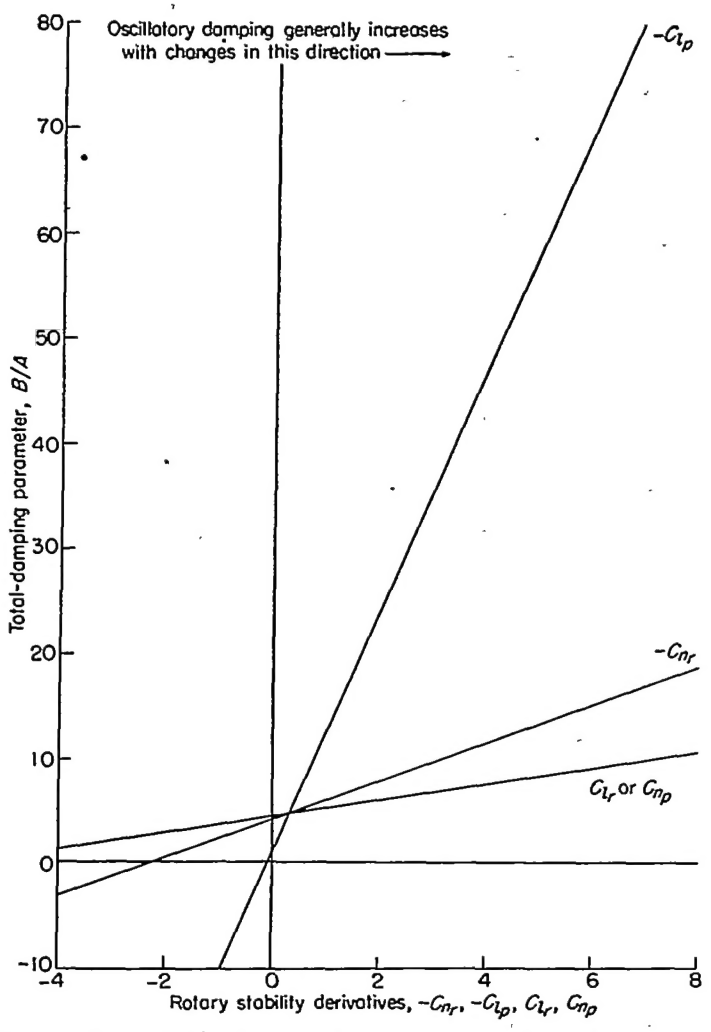

FIGURE 19.—Calculated effect of rotary stability derivatives on total damping.

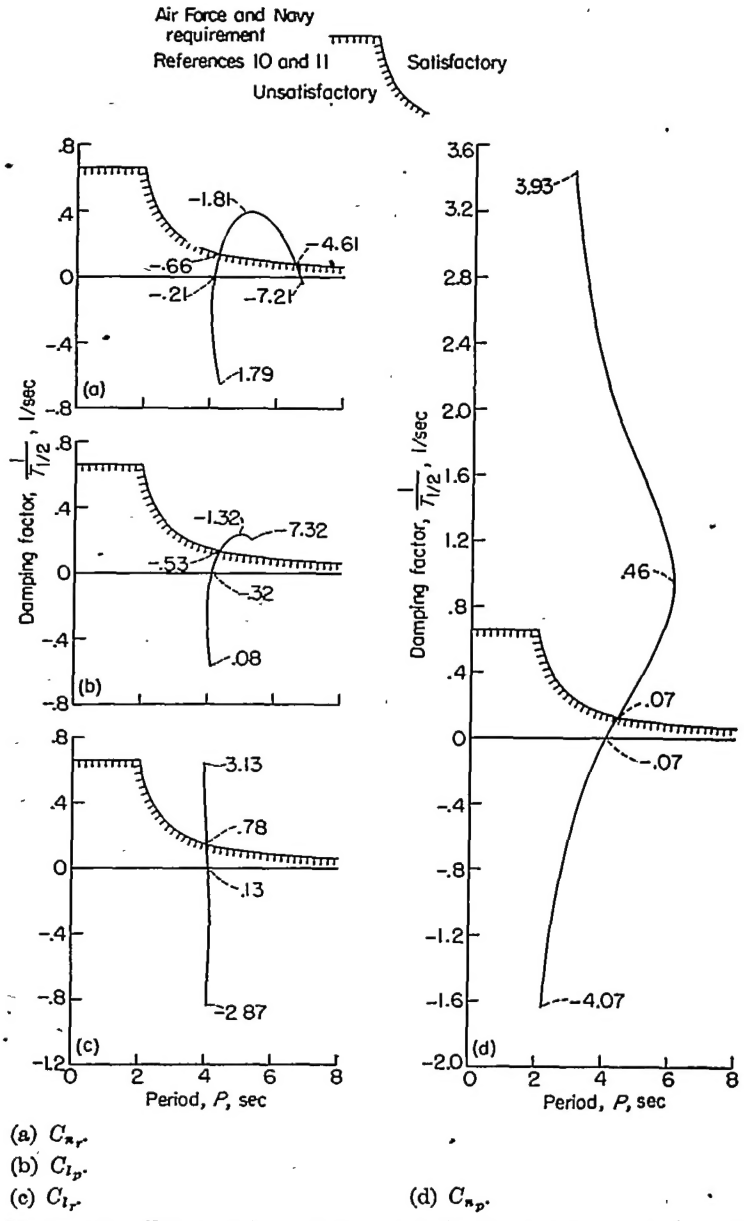

(a) C_{n_r}.
(b) C_{l_p}.
(c) C_{l_r}.
(d) C_{n_p}.

FIGURE 20.—Effect of change in rotary derivatives on damping of lateral oscillation and comparison with Air Force and Navy requirement.

as effective as increasing C_{l_p}, and increasing C_{l_r} or C_{n_p} in the positive direction was about one-fourteenth as effective as increasing C_{l_p}. Examination of the coefficient B of the quartic equation indicates that the differences in the effects of the derivatives on the total damping are directly related to the differences in the inertia parameters K_Z^2, K_X^2, and K_{XZ}. Because of this relationship the ratio of the changes of total damping is merely a reflection of the ratio of the inertia parameters; that is, K_Z^2 is approximately 7 times K_X^2 and 14 times K_{XZ}.

Although changes in the values of the cross derivatives did affect the total damping of the system, these changes primarily caused a redistribution of the damping between the various lateral modes. These effects are important when possible combinations of derivatives are being considered for improving the damping of the lateral oscillation without adversely affecting the stability of the aperiodic modes. Such a balance of stability may be accomplished by artificially increasing one of the damping derivatives and then varying the proper cross derivative to provide the desired distribution of the damping between the various lateral modes.

Comparison with Air Force and Navy damping requirements.—In order to evaluate the effectiveness of the individual rotary derivatives in improving the damping of

the oscillation for a full-scale airplane, the calculated damping has been compared with the Air Force and Navy damping requirements. (See refs. 10 and 11.) In this comparison (presented in fig. 20) the period and the damping factor have been scaled up so that the results can be compared directly with the damping requirements. In scaling up these values the model was assumed to be a $\frac{1}{9}$-scale model of an airplane; therefore, the period of the model was multiplied by 3 and the damping factor was divided by 3.

These results indicate that, in order to satisfy the requirements, C_{n_r} would have to be changed from -0.21 to -0.66, C_{l_p} from -0.32 to -0.53, C_{l_r} from 0.13 to 0.78, or C_{n_p} from -0.07 to 0.07. A brief analysis has indicated that (if lag and nonlinearities are neglected) any of these changes can be obtained with an artificial-stabilization system utilizing conventional-size control surfaces. It should be emphasized, however, that no general conclusions should be drawn from these results since they are for one airplane and one flight condition.

A comparison of figures 18 and 20 indicates that increasing any of the derivatives except C_{l_r} increased the damping enough to meet the Air Force and Navy requirements before the general flight behavior became unsatisfactory for some other reason. Another important point that can be seen in the comparison of figures 18 and 20 is that the apparent superiority of the derivative C_{n_p} in providing damping of the lateral oscillation was not realized because of the severe apparent spiral instability that resulted with large positive values of this derivative.

SUGGESTIONS FOR FUTURE RESEARCH

The present report covers a part of an investigation to determine the best means for improving the dynamic lateral stability of airplanes by means of artificial-stabilization systems. This phase was concerned primarily with the independent variation of the four rotary stability derivatives. Another phase of the investigation should be concerned with the use of combinations of these derivatives because it appears possible to increase the total damping of the system with one of the damping derivatives and then to redistribute this damping to the various lateral modes by means of a cross derivative in order to obtain good oscillatory stability without impairing the other flight characteristics.

The present investigation was concerned with pure changes in the four rotary derivatives. Since practical artificial-stabilization systems will have a certain amount of lag and nonlinearities, they cannot produce pure changes in the derivatives. Preliminary calculations indicated that appreciable changes in stability may be caused by time lag in the artificial-stabilization system. A study should therefore be undertaken to determine the ways in which the results of the present investigation would be altered by the introduction of these additional factors.

The results presented in the present report are for only one particular configuration and for one flight condition. Similar results for this and other configurations for a wide range of flight conditions should be obtained since the effects of artificial stabilization may vary widely with changes in the basic conditions.

CONCLUSIONS

The results of the investigation to determine the effects on dynamic lateral stability and control of large artificial variations in the rotary stability derivatives may be summarized as follows. Although these results do not apply directly to airplanes or flight conditions other than those investigated, the trends of the results presented are believed to provide a qualitative indication of the general effects of large variations of the stability derivatives.

1. The calculated results were in qualitative agreement with the experimental results in predicting the general trends in flight characteristics produced by large changes in the stability derivatives, but in some cases the calculations in which time lag was neglected were not in good quantitative agreement with the experimental results. In these cases, check calculations made by taking into account time lag indicated that these discrepancies could be attributed to the effect of the small constant time lag in the stabilization device used.

2. The only derivative which provided a large increase in damping of the lateral oscillation without adversely affecting other flight characteristics was the yawing moment due to yawing C_{n_r}. Because of the limitations imposed by the relatively small size of the test section of the Langley free-flight tunnel, however, the flight characteristics of the model were not appreciably influenced by the stiffness in turning maneuvers which has been found objectionable in some airplanes equipped with yaw dampers. Oscillatory instability was produced by extreme increases in C_{n_r} in the normally stabilizing direction (negative direction).

3. Increasing the rolling moment due to rolling C_{l_p} to moderately large negative values produced substantial increases in the damping of the lateral oscillation but caused an objectionable stiffness in roll. Further negative increases in C_{l_p} did not cause additional increases in the damping of the lateral oscillation and made the stiffness in roll more objectionable.

4. Increasing the rolling moment due to yawing C_{l_r} in the positive direction produced an increase in the damping of the lateral oscillation but caused an undesirable spiral tendency.

5. Increasing the yawing moment due to rolling C_{n_p} in the positive direction produced a greater increase in the damping of the lateral oscillation than that produced by any other derivative but it caused an undesirable spiral tendency before adding a substantial amount of damping.

Some preliminary calculations have indicated that the use of combinations of derivatives such as C_{n_p} and C_{l_p} or C_{n_r} and C_{l_r} should be more satisfactory than the use of single derivatives for increasing the damping of the lateral oscillation without impairing other flight characteristics.

LANGLEY AERONAUTICAL LABORATORY,
NATIONAL ADVISORY COMMITTEE FOR AERONAUTICS,
LANGLEY FIELD, VA., *June 20, 1952.*

REFERENCES

1. Sternfield, Leonard: Effect of Automatic Stabilization on the Lateral Oscillatory Stability of a Hypothetical Airplane at Supersonic Speeds. NACA TN 1818, 1949.
2. Gates, Ordway B., Jr.: A Theoretical Analysis of the Effect of Several Auxiliary Damping Devices on the Lateral Stability and Controllability of a High-Speed Aircraft. NACA TN 2565, 1951.
3. Sternfield, Leonard, and Gates, Ordway B., Jr.: A Theoretical Analysis of the Effect of Time Lag in an Automatic Stabilization System on the Lateral Oscillatory Stability of an Airplane. NACA Rep. 1018, 1951. (Supersedes NACA TN 2005.)
4. Gates, Ordway B., Jr., and Schy, Albert A.: A Theoretical Method of Determining the Control Gearing and Time Lag Necessary for a Specified Damping of an Aircraft Equipped With a Constant-Time-Lag Autopilot. NACA TN 2307, 1951.
5. Shortal, Joseph A., and Osterhout, Clayton J.: Preliminary Stability and Control Tests in the NACA Free-Flight Wind Tunnel and Correlation With Full-Scale Flight Tests. NACA TN 810, 1941.
6. MacLachlan, Robert, and Letko, William: Correlation of Two Experimental Methods of Determining the Rolling Characteristics of Unswept Wings. NACA TN 1309, 1947.
7. Bird, John D., Jaquet, Byron M., and Cowan, John W.: Effect of Fuselage and Tail Surfaces on Low-Speed Yawing Characteristics of a Swept-Wing Model as Determined in Curved-Flow Test Section of the Langley Stability Tunnel. NACA TN 2483, 1951. (Supersedes NACA RM L8G13.)
8. Sternfield, Leonard: Effect of Product of Inertia on Lateral Stability. NACA TN 1193, 1947.
9. Campbell, John P., and McKinney, Marion O.: Summary of Methods for Calculating Dynamic Lateral Stability and Response and for Estimating Lateral Stability Derivatives. NACA Rep. 1098, 1952. (Supersedes NACA TN 2409.)
10. Anon.: Flying Qualities of Piloted Airplanes. USAF Spec. No. 1815–B, June 1, 1948.
11. Anon.: Specification for Flying Qualities of Piloted Airplanes. NAVAER SR–119B, Bur. Aero., June 1, 1948.
12. White, Roland J.: Investigation of Lateral Dynamic Stability in the XB–47 Airplane. Jour. Aero. Sci., vol. 17, no. 3, Mar 1950, pp. 133–148.